INFLUENCE OF SOLIDIFICATION STRUCTURE ON HOT WORKABILITY OF AN AUSTENITIC STAINLESS STEEL CONTAINING 1.1 MASS% BORON

M. Oikawa, Y. Ikegami

Nippon Yakin Kogyo CO, Japan

Abstract

This investigation has been performed to clarify the influence of the solidification structure on the hot workability of an austenitic stainless steel containing 1.1 mass% boron. The hot workability of four kinds of materials, namely, the CC slab, the plate made from the CC slab, the ingot and the plate made from the ingot, was estimated by the reduction of area at fracture through hot tensile test in the temperature range from 1200℃ to 800℃, and microstructural observation of these materials before and after hot tensile test was conducted by optical microscopy mainly. The results indicate that the solidification structure, especially the size of boride, strongly affects the hot workability of an austenitic stainless steel containing 1.1 mass% boron, and the finer solidification structure causes the superior hot workability not only in the as-cast condition but also in the as-forged condition.

Introduction

High-boron containing austenitic stainless steels are used on storage racks and transportation components for spent fuels in the nuclear power industry because of their good neutron absorptionability and high corrosion resistance.[1] The addition of natural boron with 20% of the neutron absorbing isotope ^{10}B, increases the neutron absorptionability of these steels. However, the addition of boron deteriorates the hot workability of these steels, since boron combines with iron and chromium to form a hard and brittle boride, approximating to $(Fe,Cr)_2B$,[2] during eutectic solidification process because of the low solubility of boron in these steels. Quite many researchers have investigated the influence of alloying elements and hot working process conditions on the hot workability of these steels.[3-6] On the other hand, little systematic study on the influence of the solidification structure has been done.[7]

In this study, we investigated the hot ductility of austenitic stainless steels containing 1.1 mass% boron made through two kinds of conventional casting method such as continuous casting and ingot casting, and discussed the influence of the solidification structure on the hot workability of these steels.

Experimental procedure

The chemical composition of the steel, one of the typical types in Japan[8], is shown in Table 1.

Table1. The chemical composition of the steel (wt%)

C	Si	Mn	Cr	Ni	B
0.02 ~ 0.03	0.8 ~ 0.9	0.9 ~ 1.0	18.3 ~ 19.6	10.2 ~ 10.3	1.1

A slab produced by continuous casting (CC slab) [9] and a ingot produced by an up-hill mold were forged into plate at 1150℃ with a reduction of about 60%. The test specimens were taken from four kinds of materials, namely, the CC slab, the plate made from the CC slab, the ingot and the plate made from the ingot.

The microstructural observations of all kinds of specimens before tensile test were conducted by optical microscopy. For some fractured specimens, microstructure was examined by both optical microscopy and transmission electron microscopy. The hot workability in the temperature range from 1200℃ to 800℃ was estimated by the reduction of area at fracture through hot tensile test using a thermo mechanical simulator. The specimens for test from 1200℃ to 1000℃ had the diameter of 5 mm, while the specimens for test at 900℃ and 800℃ had the diameter of 3 mm. The constant cross head speed was 100 mm/s , corresponding to an initial strain rate of approximate 5 s^{-1}.The specimen was heated to 1150℃, held for 60s followed by cooled down to the test temperature, kept for 60s, and tensile tested. For the estimation of hot workability at 1200℃, the specimen was heated to 1200℃, held for 60 s, and then tensile strained.

Results and discussion

Figure 1 shows the microstructure of all materials before tensile test.

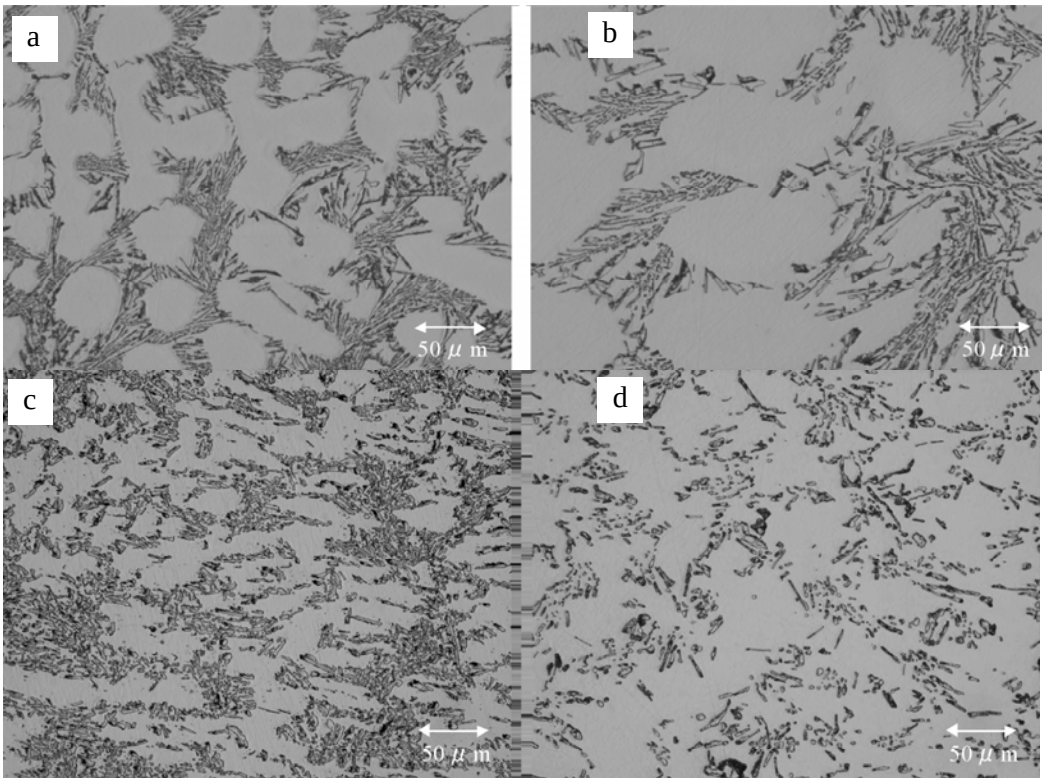

Figure 1. The microstructure of all materials before tensile test
(a) the CC slab (b) the ingot (c) the plate made from the CC slab (d) the plate made from the ingot

The microstructure of both the as-cast CC slab and the as-cast ingot consisted of primary dendrites of austenitic phase and eutectoids of austenitic phase and boride, and the as-cast CC slab had finer eutectoids than the as-cast ingot. EPMA analysis showed the borides were $(Fe,Cr)_2B$ as other researchers have reported.[2] These microstructural features revealed that the cooling rate of the CC slab was faster than that of the ingot although both materials solidified through the same mode.

Also, it was found that the eutectic structure was broken down and fine borides were distributed uniformly in the austenitic matrix through the forging process, and the plate processed from the CC slab with finer solidification structure had smaller borides than the plate made from the ingot.

The curves of hot ductility as a function of test temperature are presented in Figure 2.

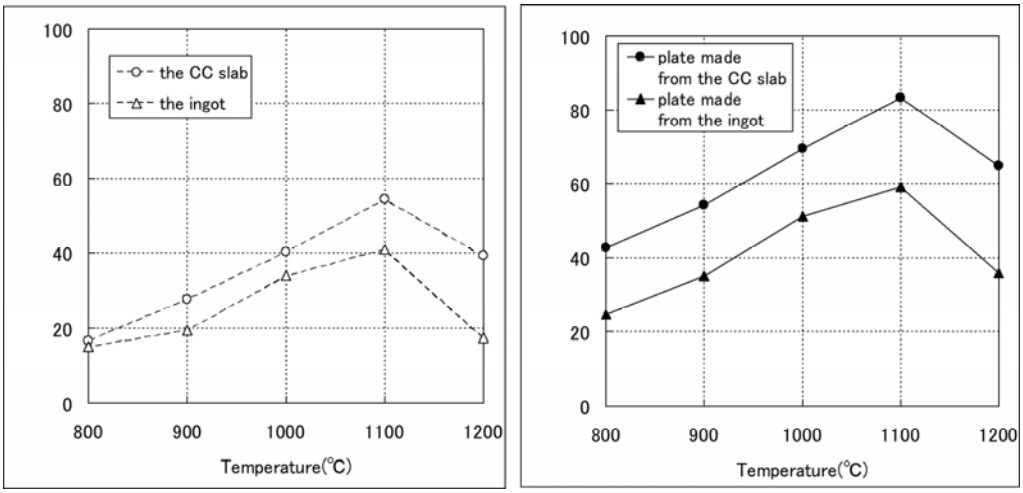

Figure 2. The hot workability of all materials

The temperature dependence of the hot workability for all materials shows a similar trend, i.e., with increasing temperature, hot workability increases reaching the maximum value at 1100°C followed by a drop. Low values at 1200°C are thought to be related to the eutectic point of 1250°C.[10] The as-cast CC slab that has finer eutectoid than the as-cast ingot, has hot workability superior to the as-cast ingot at all testing temperatures.

The forging process improves the hot workability of the materials manufactured by both casting method, and the plate made from the CC slab, which has smaller borides, has superior hot workability.

Some investigators have described that by the forging process, borides became finer and hot workability was improved. But they did not confirm whether the solidification structure affected the hot workability of forged plate or not, because they have studied the materials made employing one kind of the casting method only.[1,5]

As mentioned above, it is revealed that the solidification structure, especially the size of borides, strongly affects the hot workability of an austenitic stainless steel containing 1.1mass% boron, and the finer solidification structure causes the superior hot workability not only in the as-cast condition but also in the as-forged condition.

To investigate the influence of the solidification structure on the hot workability in more detail, we observed the microstructure of the fractured specimens by optical microscopy and transmission electron microscopy (TEM).

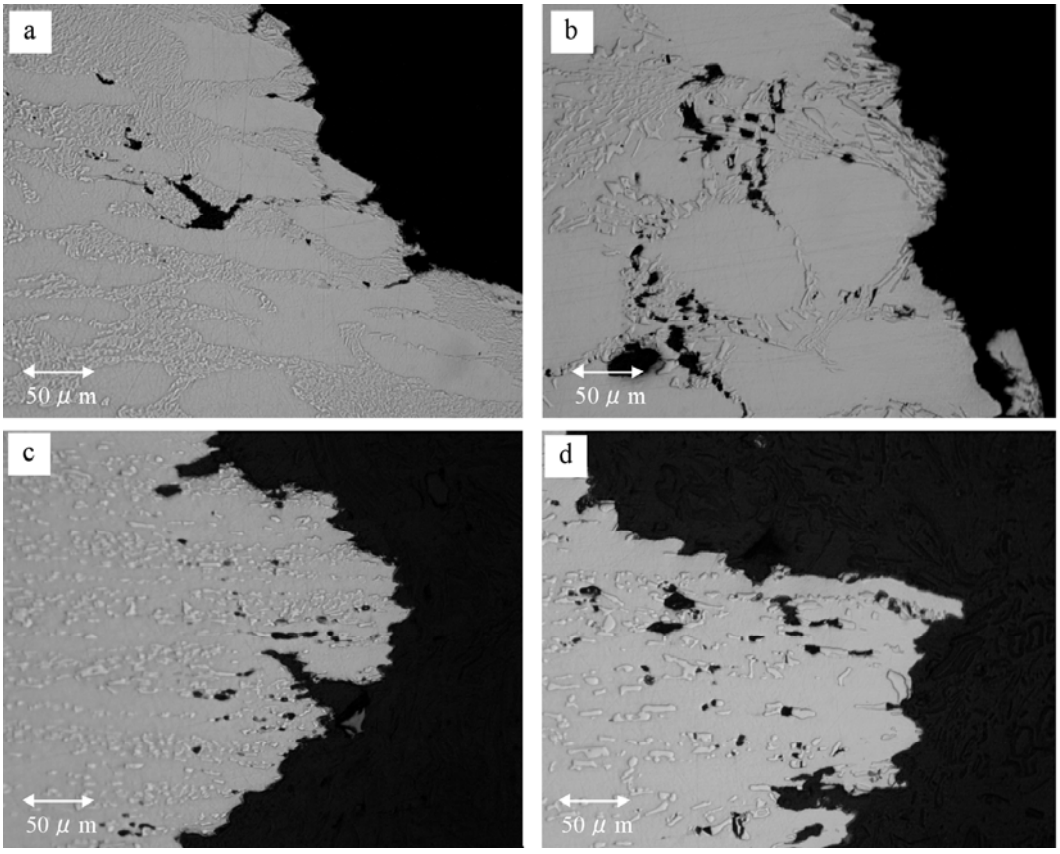

Figure 3. The microstructure of four kinds of specimens fractured at 1000°C
(a) the CC slab (b) the ingot (c) the plate made from the CC slab (d) the plate made from the ingot

Figure 3 shows the microstructure of four kinds of specimens fractured at 1000℃. Cracks initiated at the interface between the austenitic matrix and the eutectic structure consisting of the austenitic phase and borides, or the interface between the austenitic phase and borides, and then cracks were linked and propagated mainly along these interfaces.

Figure 4 shows the TEM micrographs of the part about 4mm away from the fracture surface of the CC slab specimens deformed at 1000°C. The reduction of area of the observed part was estimated to be about 20% by measurement of the diameter. As shown in Figure 4(a), the dislocation cell structure appeared in the austenitic phase near the eutectoid whereas the austenitic phase in the eutectoid had low dislocation densities. This microstructure indicates that hard borides suppress the deformation of the austenitic phase in the eutectoid, and stress concentrates at the interface between the austenitic matrix and the eutectic structure during tensile deformation. Also, some recrystallized grains were observed at the interface between the austenitic phase and borides, as shown in Figure 4(b). This micrograph suggestes that strain concentrates to the interface between the austenitic phase and the hard boride.

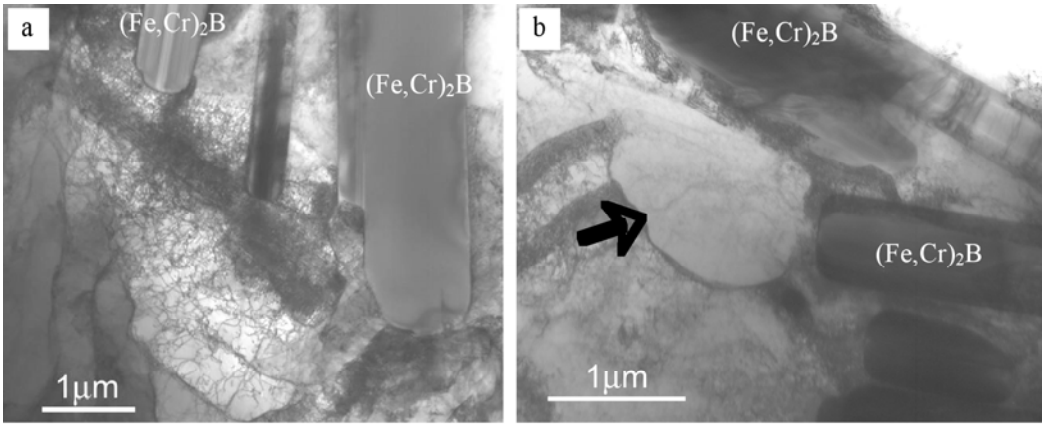

Figure 4. TEM micrograph of the CC slab speimen deformed about 20% at 1000°C
(a) the cell structure in the austenitic phase near the eutectoid
(b) the recrystallized grain at the interface between the austenitic phase and the eutectoid

From the observation above, the fracture mechanism of these steels is considered as follows: during deformation of the as-cast materials, stress concentrates easily at the interface between the austenitic matrix and the eutectoid because hard borides suppress the deformation of the eutectoid. Voids nucleate at the interface between the austenitic matrix and the eutectoid, and then coalesce, leading to macroscopic fracture. On the as-forged materials with uniformly dispersed borides, voids nucleate at the interface between the austenitic phase and the hard boride, and grow, leading to fracture.

Because the morphology of borides, especially the size of borides, affects the local deformation at the regions near the eutectoid and the stress concentration at the interface between the austenitic phase and the boride, the solidification structure strongly affects the hot workability of these steels.

On the basis of the understanding of the effect of the solidification structure on hot workability of the austenitic stainless steel containing 1.1mass% boron, the mass production of coil products of these steels has been done successfully through continuos casting process.[9]

Conclusions

In this study, we investigated the hot ductility of an austenitic stainless steels containing 1.1mass% boron made through two kinds of conventional casting method such as continuous casting and ingot casting, and discussed the influence of solidification structure on hot workability of these steels. The following results are obtained:

- The microstructure of both the as-cast CC slab and the as-cast ingot consisted of primary dendrites of austenitic phase and eutectoids of austenitic phase and boride, and the as-cast CC slab had finer eutectoids than the as-cast ingot. The as-cast CC slab had hot workability superior to the as-cast ingot.
- Through the forging process, the eutectic structure was broken down and fine borides were distributed uniformly in the austenitic matrix, and hot workability was improved. The plate made from the CC slab with finer solidification structure had smaller borides and superior hot workability.
- It is revealed that the solidification structure, especially the size of borides, strongly affects the hot workability of the austenitic stainless steel containing 1.1mass% boron, and the finer solidification structure results in the superior hot workability not only in the as-cast condition but also in the as-forged condition.

References

[1] K.J. King and J. Wilkinson: Stainless Steel ’84, The Institute of Metals, UK, 1984, pp. 368 – 378

[2] T. Nishima: “Effect of B, C, Ni and Cr Contents on Properties of Boron Stainless Steel”, Tetsu to Hagane, Vol. 48, No. 11, 1962, pp. 1495 – 1496

[3] T. Nishima: “Effect of Some Alloyng Elements on Properties of Boron Stainless Steel”, Tetsu to Hagane, Vol. 48, No. 11, 1962, pp. 1496 – 1498

[4] R. Nemoto: Stainless Steel 93, Associazione Italiana Di Metallurgia, Italy, 1993, pp. 1.195 – 1.200

[5] K. Yamasaki, Y. Kawai and T. Takemoto: Stainless Steel 93, Associazione Italiana Di Metallurgia, Italy, 1993, pp. 1.85– 1.90

[6] H. Morikawa, O. Yamamoto and T. Takemoto: “Effects of Hot-Rolling Temperature and Reduction Ratio on Edge Cracking of Hot-Rolled Boron-Containing Stainless Steel”, CAMP-ISIJ, Vol. 11, No. 3, 1998, pp. 588

[7] M. Oikawa, Y. Fujiwara and T. Touge: “Effects of Microstructure on Hot Workability of Hypo-eutectic Boronated Stainless Steel”, CAMP-ISIJ, Vol. 9, No. 6, 1996, pp. 1238

[8] M. Tsubota and M. Oikawa: “Boron-bearing Stainless Steels for Thermal Neutron Shielding” Bulletin of The Iron and Steel Institute of Japan, Vol. 10, No. 12, 2005, pp. 25 – 27

[9] T. Ishii, H. Todoroki, M. Oikawa, K. Mizuno, A. Hongou and A. Tanaka: “Continuous Casting Technology of Stainless Steel Containing Boron”, CAMP-ISIJ, Vol. 4, No. 1, 2001, pp. 162

[10] M. Oikawa and Y. Fujiwara: Nippon Yakin Gihou, Nippon Yakin Kogyo, Japan, No. 6, 1997, pp. 10 – 18.

APPLICATION OF THERMOELECTRIC POWER MEASUREMENTS TO THE STUDY OF COLD ROLLED AISI 304 STEELS

T. De Cock[1], C. Capdevila[1], F.G. Caballero[1], D. San Martín[2], C. García de Andrés[1]

[1]Centro Nacional de Investigaciones Metalúrgicas (CENIM), Consejo Superior de Investigaciones Científicas (CSIC), Spain, [2]Delft University of Technology, The Netherlands

Abstract

The influence of the deformation grade on the recrystallised grain size has been studied in AISI 304 stainless steel. Therefore, cold rolled samples of this material with reductions varying between 30% and 80% were annealed at different temperatures and subsequently quenched. At each stage the recrystallised austenitic grain sizes were compared with the thermoelectric power measurements. Moreover, a chemical etching procedure was developed in order to reveal the presence of a second phase precipitated at the austenitic grain boundaries. It was observed that this second phase precipitation plays an important role in the recrystallisation process. Finally, the combined study of the dissolution of those precipitates at different annealing temperatures and the corresponding thermoelectric power measurements allowed to describe the recrystallisation behaviour of this type of stainless steels for each prior cold rolling degree.

Introduction

Austenitic stainless steels AISI 304 are widely used steels combining high corrosion-oxidation resistance, good heat resisting properties and a relative low cost. However, one of the main drawbacks of these steels is their low mechanical resistance obtained in standard production processes. Therefore, in recent years an increasing interest can be noted in the development of new processing routes. One of the key issues in this field is the study of the microstructural evolution of the cold-rolling material at different annealing temperatures.
In this context, the aim of the work presented in this paper was to characterise the recrystallised grain growth of the AISI 304 steels annealed at temperatures between 1000 and 1200 ºC and for different rolling reductions, using thermoelectic power (TEP) measurements.

Experimental procedure

The chemical composition of the studied steel in wt% is as follows: 0.039% C, 0.22% Si, 0.001% S, 0.029% P, 1.15% Mn, 18.0% Cr, 8.52% Ni, 0.24% Mo, 0.25% Cu, 0.0005% B, and 0.04% N. The material was obtained from a hot-rolled coil and was subsequently cold rolled down to 30%, 70% and 80% reduction. In order to study the evolution of the recrystallised grain growth, samples 30 mm in length, 2 mm in width and 0.8 mm in thickness were annealed at different temperatures (1000, 1050, 1100, 1150 and 1200°C). After 180 seconds of holding time, specimens were rapidly cooled to room temperature. These heat treatments were appropriately chosen in order to obtain fully recrystallised samples in each case.

The samples were etched with a solution containing 60% hydrochloric acid, 20% nitric acid and 20% methanol to reveal the individual grains. The micrographs were then analysed with the Image Tool 2.0 software. To study the presence of second phases, these samples where repolished and then etched with the Lichtenegger-Bloch reagent [1], which consists of 20 g ammonium difluoride, 0.5 g potassium bisulfite and 100 ml hot distilled water.

A schematic representation of the TEP apparatus is given elsewhere [2-4]. The experimental procedure of the TEP measurement is the following: the sample is pressed between two blocks of a reference metal (in this case, pure copper). One of the blocks is at 15°C, while the other is at 25°C to obtain a temperature difference ΔT. A potential difference ΔV is generated at the reference metal contacts. The apparatus does not give the absolute TEP value of the sample (S^*), but a relative TEP (S) in comparison to the TEP of pure copper (S_0^*) at 20°C. S is given by $S = S^* - S_0^* = \Delta V/\Delta T$. The TEP value does not depend on the shape of the sample, which is a great advantage of this technique. Moreover, the measurement is performed very quickly (less than 1 min) and precisely (about ± 0.5%). The resolution is of the order of 0.001 μV/K.

Results and Discussion

As an example, Figure 1 shows the optical micrographs of the annealed microstructures with increasing annealing temperature for the case of 30% deformation.

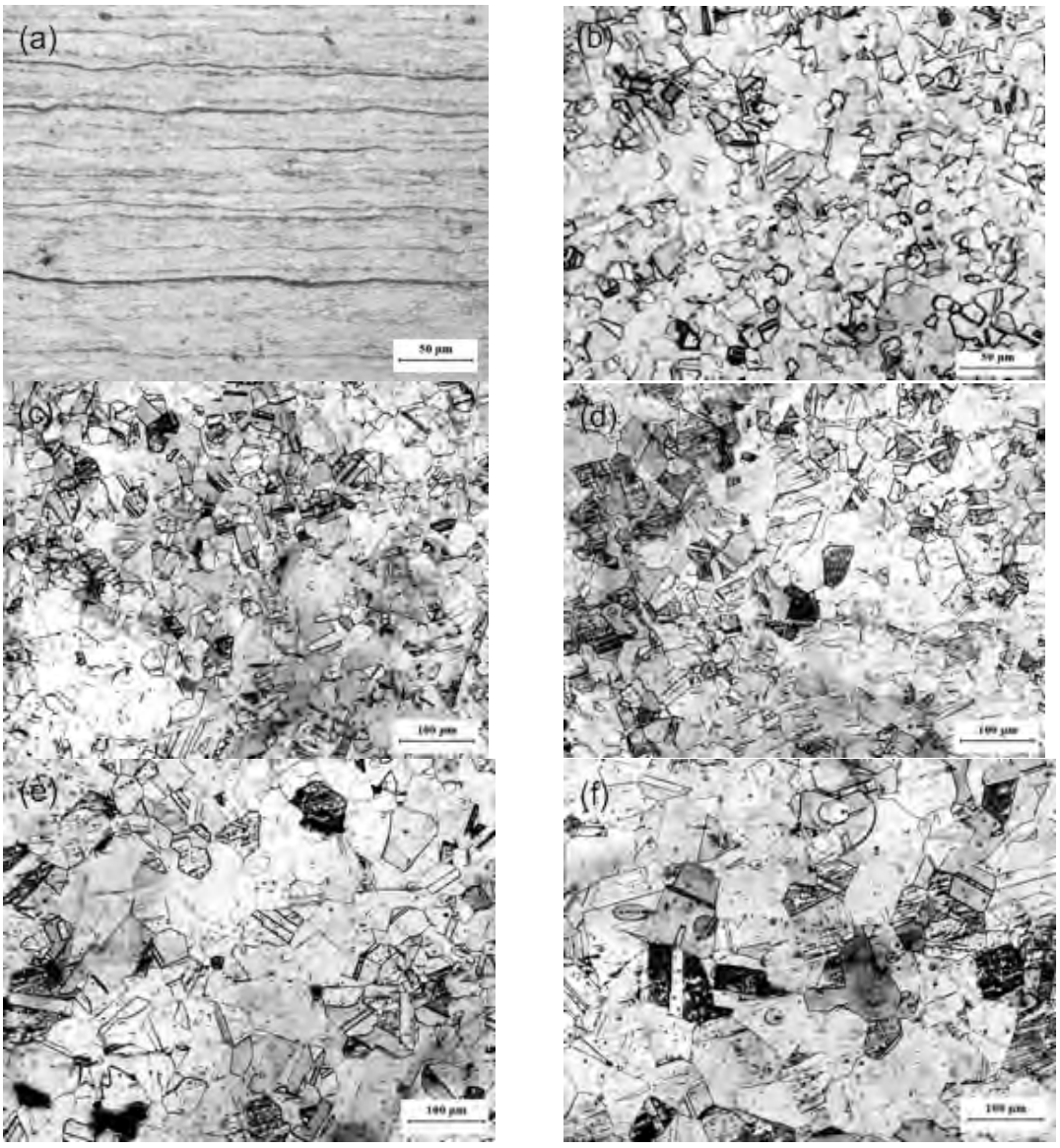

Figure 1. Optical micrographs of the AISI 304 steel with 30% rolling reduction (a) in the as-cold rolled condition and after heat treatment at (b) 1000ºC, (c) 1050ºC, (d) 1100ºC, (e) 1150ºC and (f) 1200ºC.

The applied etching procedure enables to reveal the evolution of the recrystallised grain size (expressed as the average grain diameter) with the annealing temperature, which has been measured for each degree of deformation. This is shown in Figure 2. Subsequently, for each annealing stage the corresponding TEP value was measured, taking the TEP value at the lowest annealing stage (i.e. at 1000ºC) as a reference level for each deformation level. The results of the TEP analysis is given in Figure 3.

From comparison between Figures 2 and 3, it can be seen that the faster kinetics for higher deformed material (70 and 80%) leads to higher recrystallised grain sizes and higher values of TEP compared to the case of small deformation (30%). Whereas at higher temperature a clear influence of the grain growth can be noted on the TEP values, especially in the highly deformed steels, the negative values of the TEP at lower holding temperatures and at lower deformation degrees of deformation indicate that the TEP measurement in these cases is dominated by other effects than recrystallised grain growth, e.g. dissolution processes.
The presence of delta ferrite as a second phase in AISI 304 has been broadly reported [5]. To study the possible influence of a second phase, the samples were etched with the Lichtenegger-Bloch reagent. As can be seen in Figure 4, the low deformed steel contains delta ferrite phase, which is known to constitute a preferential nucleation site for $M_{23}C_6$ particles [6], primarily at the δ/γ interface. Since during annealing at high temperatures these particles dissolve very rapidly, the solute content of elements such as C and Mn increases, which explains the negative TEP values. At high deformation levels, no delta ferrite was detected, and thus the dissolution mechanism does not apply in this case, leading to high TEP values. The behaviour of the steels with deformation degrees of 70 and 80% is very similar, except for low and high annealing temperatures: at low annealing temperatures a small influence of dissolution processes in the steel with cold rolling degree of 70% is observed, whereas at high annealing temperatures the average recrystallised grain size of the 70% is slightly higher than for 80% steels. The lower grain growth at this stage for the steel with 80% deformation is probably related with additional solute drag phenomena. This is also in agreement with the corresponding TEP measurements, as can be seen in Figure 3.

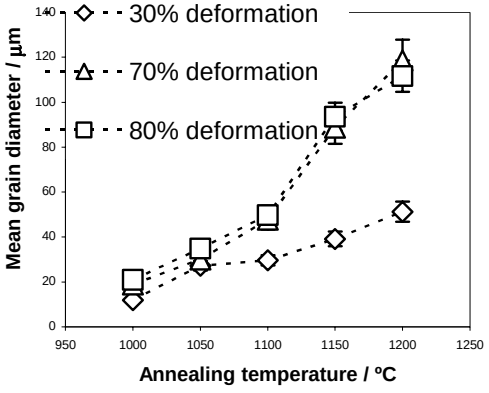

Figure 2. Evolution of the recrystallised grain size for the three cold rolling reductions

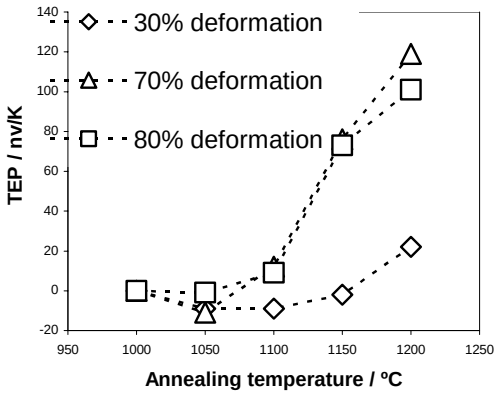

Figure 3. Evolution of the thermoelectric power for the three cold rolling reductions

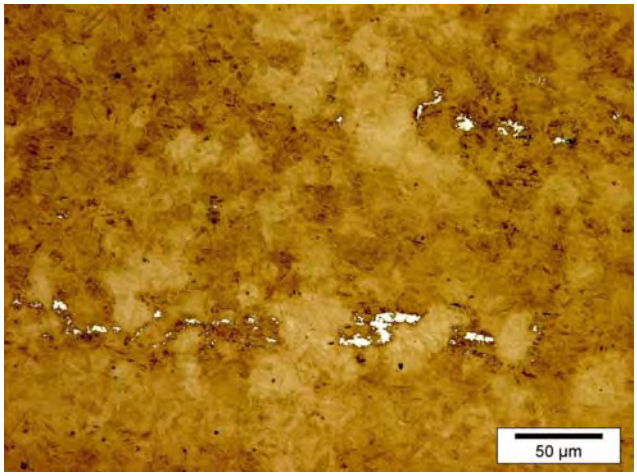

Figure 4. Lichtenegger-Bloch etch of the sample deformed at 30% and after annealing at 1000ºC. The white phase corresponds to delta ferrite, the brown phase is the austenitic matrix.

Conclusions

The evolution of the recrystallised grain size for isothermal annealing treatments has been studied in AISI 304 stainless steels with reductions between 30 and 80%. It is observed that the increase of the grain size is still relatively limited at lower annealing stages. At these annealing stages, the contribution to the TEP measurements is dominated by the dissolution of particles. At higher annealing temperatures and higher deformations, the increase of the grain size leads to high TEP values, whereas the influence of dissolution processes is only significant in the steel with a reduction of 70% and at low annealing temperatures.

Acknowledgements

The authors acknowledge financial support from European Coal and Steel Community (ECSC-7210-PR-368) and from Spanish Ministerio de Educación (MAT2002-18810-E). CSM is acknowledged for supplying the material for this study. T. De Cock would also like to express his gratitude to the Consejo Superior de Investigaciones Científicas (CSIC) for financial support in the form of a Ph.D. research grant (I3P program).

References

[1] G. Vander Voort: Metallography Principles and Practice, 1999, ASM International, p. 649
[2] A. Ney Jose Luiggi: Metall. Mater. Trans. A 29, 1998, p. 2669
[3] C. Capdevila, T. De Cock, F. G. Caballero, C. Garcia-Mateo and C. Garcia de Andres: Materials Science Forum, 467-470, 2004, p. 863
[4] F. G. Caballero, L.F. Alvarez, C. Capdevila and C. Garcia de Andres: Scripta Materialia, 49, 2003, p. 315
[5] K. Borst and M. Pohl: Steel Research 61 (6), 1990, p. 258
[6] S.H. Kim, H.K. Moon, T. Kang and C.S. Lee: Mat. Sci. Eng. A356, 2003, p. 390

INVESTIGATION OF THE DYNAMIC TENSILE PROPERTIES OF AUSTENITIC STAINLESS SHEET STEELS USING TENSILE HOPKINSON SPLIT BAR

M. Isakov[1], J. Kokkonen[1], T. Vuoristo[1], V.-T. Kuokkala[1], J. Rämö[1], R. Ruoppa[2]

[1]Tampere University of Technology, Finland, [2]Tornio Research Centre, Outokumpu Tornio Works, Finland

Abstract

The effect of strain rate on the mechanical behavior of austenitic stainless sheet steel grades EN 1.4301 (AISI 304) and EN 1.4318 (AISI 301LN) was investigated with uniaxial tensile tests over a wide range of strain rates. Tests were performed in the low strain rate region (10^{-3} ... 1 s^{-1}) using a conventional servo-hydraulic materials testing machine, and in the high strain rate region (500 ... 1500 s^{-1}) with a Tensile Hopkinson Split Bar apparatus (THSB). Increasing strain rate increased the yield strength of both grades, but the plastic deformation behavior of the two grades differed markedly from each other. The ductility of the EN 1.4301 grade decreased notably with increasing strain rate, while the EN 1.4318 grade showed decreasing strain hardening capability with increasing strain rate. Martensite content measurements on the specimens tested until fracture showed that the final amount of strain-induced α'-martensite decreases with increasing strain rate. Tests carried out at different temperatures for the EN 1.4318 grade demonstrated that the effects of strain rate depend also on the initial test temperature.

Introduction

Both strain rate and temperature have a strong effect on the mechanical behavior of most materials. In crystalline materials, these effects are usually explained by thermally activated dislocation motion, but also the microstructure may evolve differently depending on the loading conditions, i.e., rate of loading, initial temperature of the material, and stress state. The need to understand material behavior in demanding applications and the increasing use of FE-simulations in the design of products and processes also call for accurate and reliable material data over wide ranges of temperature and strain rate.

Austenitic stainless steels have gained wide use in the industry due to their excellent corrosion resistance and good mechanical properties. The metastable nature of the austenite phase introduces interesting features into the mechanical behavior of these materials. The strain-induced austenite-to-martensite ($\gamma \rightarrow \alpha'$) transformation, which is partly responsible for the good mechanical properties of austenitic stainless steels, is significantly affected by both strain rate and temperature. Tests made at different temperatures at low strain rates have shown that the transformation rate increases with decreasing temperature and that the shape of the tensile stress-strain curve of the material changes from the typical parabolic to sigmoidal[1, 2]. In contrast to the continuously decreasing strain hardening rate related to the parabolic stress-strain curve, the sigmoidal curve shows a distinct minimum in the strain hardening rate followed by a rapid increase and a maximum, after which the strain hardening rate decreases again before the onset

of tensile instability, i.e., necking[3]. According to Huang et al.[3], the uniform elongation has a maximum at a certain temperature, where the α'-martensite transformation persists to high strains, keeping the strain hardening rate high enough to efficiently delay necking. High strain rate tests performed at room temperature have indicated that although increasing strain rate may promote the austenite-to-martensite transformation[1, 4], the total amount of transformed α'-martensite decreases at high strain rates due to adiabatic heating[1, 2, 5]. Talonen[2], who compared the room temperature tensile behavior of stainless steels AISI 304 and AISI 301LN at strain rates up to 200 s^{-1}, found that increasing strain rate reduced the ductility of the more stable 304-grade, while the strain hardening rate maximum of the unstable 301LN-grade was lowered and shifted to higher strains. However, more experimental data is needed on the combined effects of high strain rate and varying test temperature.

Tensile Hopkinson Split Bar (THSB) technique is practically the only reliable method to study the uniaxial dynamic tensile behavior of materials near and above the strain rate of 1000 s^{-1}. In this work, austenitic stainless sheet steels EN 1.4301 (AISI 304) and EN 1.4318 (AISI 301LN) were investigated using the THSB apparatus in the high strain rate region 500 ... 1500 s^{-1}. The results of these tests were compared with conventional tensile test results in the low strain rate region 10^{-3} ... 1 s^{-1}. Combined effects of strain rate and temperature were studied with a high/low temperature THSB system, and with temperature controlled low strain rate tensile tests. Martensite contents were measured from the specimens deformed until fracture with a portable ferrite measurement device[6].

Experimental methods

Tensile Hopkinson Split Bar

Tests in the high strain rate region 500 ... 1500 s^{-1} were carried out with the Tensile Hopkinson Split Bar (THSB) method. Figure 1a presents schematically the THSB apparatus used at the Department of Materials Science of Tampere University of Technology. The apparatus consists of two long bars, the incident and transmitted bars, between which the specimen is mounted, and of a striker tube, which is placed around the incident bar. The specimen is fixed with a cyanoacrylate adhesive into the slits machined to the ends of the bars. Tensile load is created by shooting the striker with compressed air against a flange at the far end of the incident bar. The impact creates a wave of tension, which propagates in the incident bar until it reaches the specimen-bar interface, where part of the wave is reflected back as a wave of compression, while the rest of it propagates through the specimen to the transmitted bar as a wave of tension. These three elastic waves are measured with strain gauges attached to the bars, amplified, and recorded using a digital oscilloscope. The data is downloaded to a computer, where the effects of wave dispersion are first corrected. Based on the recorded and dispersion-corrected waves, strain rate, strain, and stress in the specimen are determined as a function of time by calculating the relative movement of the bar ends (i.e., the specimen grip sections) and the longitudinal force acting on the specimen. Since the specimen is glued into the bars of the THSB apparatus, special methods have to be used to control the test temperature. These methods are described in details by Hokka et al.[7], but as a brief description, heating of the specimen is accomplished with rapid contact heating by pre-heated copper blocks to prevent the glue joints from overheating, and the cooling of the specimen is achieved with cryogenic nitrogen gas flow in a cooling chamber surrounding the specimen.

Low strain rate testing

Tests in the low strain rate region (10^{-3}... 1 s^{-1}) were carried out with a servohydraulic materials testing machine Instron 8800. Temperatures below ambient were achieved with the cryogenic nitrogen gas method described above, and elevated temperature testing was done using a vertical

tube furnace. In the room temperature tests, strain was measured directly from the specimen with a 6 mm gauge length extensometer. In low and high temperature tests specimen strain was calculated from the relative movement of the grips measured by an LVDT transducer.

Materials and specimen geometry

The austenitic stainless steel grades chosen for this study were industrial quality sheet steels EN 1.4301 and EN 1.4318. Table 1 shows the chemical compositions of the studied grades. The specimen details and test temperatures are given in Table 2. The austenite in the EN 1.4301 grade was considered to be relatively stable at room temperature, whereas easy transformation from austenite to martensite was expected to occur during plastic deformation of the EN 1.4318 grade[2].

Table 1. Chemical compositions of the studied steel grades in wt-%.

Steel grade	C	Si	Mn	Cr	Ni	Mo	Cu	N	Fe
EN 1.4301-2B*	0.055	0.49	1.7	18.3	8.1	0.17	0.39	0.05	bal.
EN 1.4318-2B*	0.022	0.43	1.26	17.4	6.5	0.21	0.22	0.127	bal.
EN 1.4318-2H/C850**	0.017	0.5	1.27	17.8	6.4	0.06	0.18	0.117	bal.

*) 2B: cold rolled, heat treated, pickled, and skin passed

**) 2H/C850: 2B work hardened by additional cold rolling to standard tensile strength of 850 MPa

Table 2. Specimen details and test temperatures of the studied steel grades.

Steel grade	Thickness (mm)	Test direction	Specimen preparation	Test temperature (°C)
EN 1.4301-2B	0.80*	transverse	Milling cutter	+24
EN 1.4318-2B	1.19	transverse	Milling cutter	+24
EN 1.4318-2H/C850	2.0	transverse	CO_2-laser	-40, +24, +80

*) stacks of two specimens were used in THSB testing to improve signal quality

Figure 1b presents the specimen geometry used throughout this study. It was chosen based on an extensive experimental and numerical study by Curtze et al.[8]. In the tests where the extensometer could not be used (i.e., in THSB testing and in the low strain rate testing of EN 1.4318-2H/C850 at elevated and sub-zero temperatures), a nominal gauge length of 8 mm was used in the strain calculations.

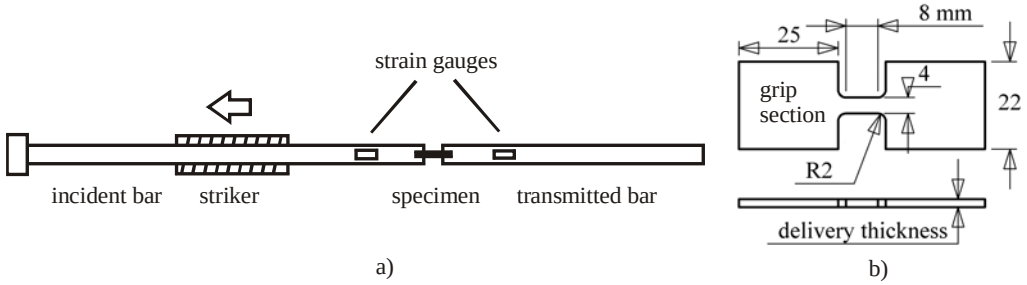

Figure 1. a) A schematic picture of the Tensile Hopkinson Split Bar apparatus used at Tampere University of Technology, and b) the specimen geometry used throughout the study.

Results and discussion

Figures 2, 3a, and 4a present the effect of strain rate on the room temperature tensile behavior of stainless steels EN 1.4301-2B and EN 1.4318-2B. The yield strength of both materials increases in a quite similar manner, i.e., almost linearly with the logarithm of increasing strain rate, but the plastic deformation behavior of the two materials differs quite notably. According to Figure 2, the more stable EN 1.4301-2B grade shows rather similar strain hardening behavior at all studied strain rates, whereas the shape of the true stress-true strain curve of the unstable EN 1.4318-2B

grade changes from sigmoidal at the low strain rate of 10^{-3} s^{-1} to almost parabolic at the high strain rate of 1000 s^{-1}, indicating that the strain hardening rate of EN 1.4318-2B is significantly reduced at higher strain rates above the true strain of 10%. The uniform elongation values presented in Figure 4a suggest that for the EN 1.4301-2B grade the uniform elongation is reduced when the strain rate is increased, while for the unstable grade the uniform elongation seems to be less affected by the strain rate. It should be noted, however, that in the THSB tests the specimen strain was calculated from the relative movement of the bar ends, and therefore the uniform elongation values at high strain rates may be slightly overestimated due to the additional strain coming from outside of the specimen gauge section.

According to Figure 3a, the ultimate tensile strength (UTS) of the unstable EN 1.4318-2B grade first decreases rapidly with increasing strain rate, reaching a minimum at around 1 s^{-1} due to its decreasing strain hardening capability, and then slightly increases again in the high strain rate region. The UTS of the stable EN 1.4301-2B grade is clearly less affected by the increasing strain rate. Figure 3b shows the effects of test temperature and strain rate on the UTS of EN 1.4318-2H. Again, the UTS first decreases and then slightly increases as the strain rate increases. The decrease of the UTS is more pronounced and continues to higher strain rates at lower temperatures. In fact, at -40°C the lowest UTS values were measured in the high strain rate region, where usually the flow stresses are clearly higher than at low strain rates. It should be noted, however, that the indicated temperatures refer only to the specimen temperature in the beginning of the test, and at high strain rates the deformation-induced heating can increase the specimen temperature notably and thereby alter the observed behavior.

To investigate the effects of strain rate and temperature on the austenite stability, the fractured specimens were inspected with a portable ferrite content measurement device (Fischer Feritscope MP30), the readings of which have been shown to be proportional to the α'-martensite content of the material[6]. Similar results were obtained also from reference measurements made using a Satmagan magnetic balance on some of the deformed specimens. The precise quantitative determination of the actual α'-martensite content proved to be quite difficult, and therefore only the relative Feritscope readings are indicated in Figure 4, which presents the results obtained from the area halfway from the actual fracture point to the grip section of the specimen. As expected, the overall martensite contents of the stable EN 1.4301-2B grade are significantly smaller than those of the unstable EN 1.4318-2B and EN 1.4318-2H grades. Increasing strain rate notably decreases the amount of transformed martensite in all grades. This is consistent with the findings of previous investigations[2, 5], according to which increasing deformation-induced heating at higher strain rates suppresses the austenite-to-martensite transformation.

As shown in Figure 4b, increasing strain rate decreases the α'-martensite content of the EN 1.4318-2H grade at all test temperatures, but the effect seems to be most pronounced in the low strain rate region at room temperature. Talonen[2] studied the evolution of α'-martensite volume fraction in EN 1.4318-2B grade as a function of strain at various temperatures at a constant strain rate of $3 \cdot 10^{-4}$ s^{-1}, and at room temperature at strain rates ranging from $3 \cdot 10^{-4}$ s^{-1} to 200 s^{-1}. A significant reduction in the martensite transformation rate and in the total amount of transformed martensite was found when temperature was increased from +40°C to +80°C at the low strain rate. Talonen also observed that the transformation rate decreased with increasing strain rate at room temperature, the effect being greater between strain rates $3 \cdot 10^{-4}$ s^{-1} and 10^{-1} s^{-1} than between 10^{-1} s^{-1} and 200 s^{-1}. Thus, based on the findings of Talonen[2] and the results presented in Figure 4b, the strain-induced austenite-to-martensite transformation of the EN 1.4318 grade seems to be particularly sensitive to the increase in temperature, either initial or deformation-induced, near and slightly above room temperature. However, the arguments

presented here are not conclusive until the evolution of the α'-martensite volume fraction under the test conditions used in this work has been studied also as a function of strain.

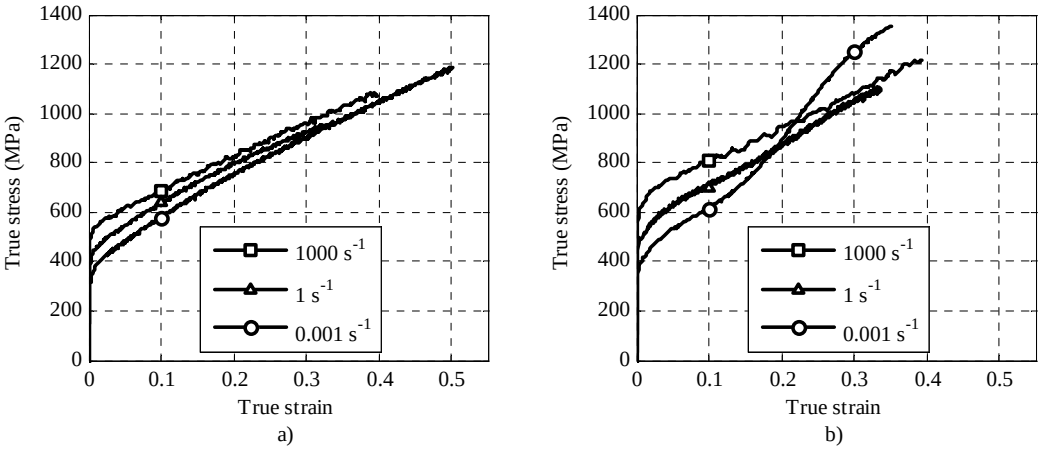

Figure 2. True stress-strain curves up to uniform elongation at various strain rates at room temperature: a) EN 1.4301-2B b) EN 1.4318-2B.

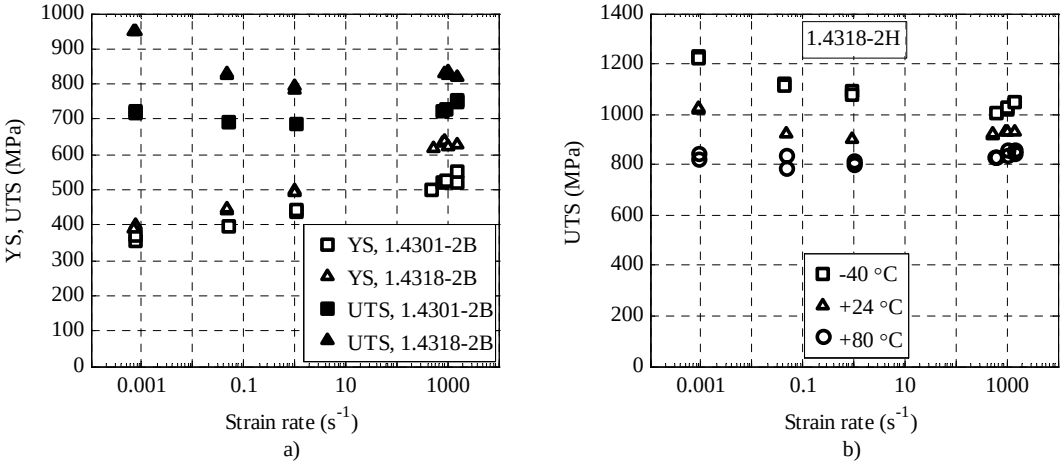

Figure 3. Influence of strain rate and temperature on strength: a) EN 1.4301-2B and EN 1.4318-2B at room temperature, yield strength (YS, $R_{p0.5\%}$) marked with open symbols and ultimate tensile strength (UTS) with filled symbols b) EN 1.4318-2H at various temperatures, UTS.

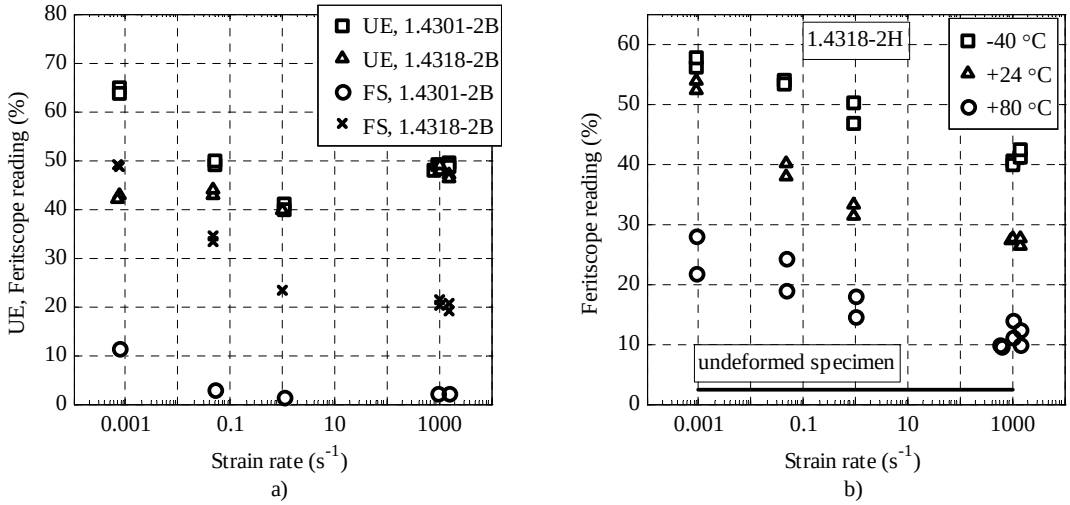

Figure 4. Influence of strain rate on a) the uniform elongation (UE) and the Feritscope readings (FS) proportional to the α'-martensite contents of EN 1.4301-2B and EN 1.4318-2B at room temperature, and b) the Feritscope readings of EN 1.4318-2H at different temperatures.

Conclusions

In this paper, the results of tensile tests for austenitic stainless steel grades EN 1.4301-2B, EN 1.4318-2B and EN 1.4318-2H/C850 are presented and discussed. Tests were carried out over wide ranges of strain rate and temperature using a conventional servo-hydraulic materials testing machine and a Tensile Hopkinson Split Bar apparatus with incorporated heating/cooling systems. The results clearly show that both strain rate and temperature have to be accounted for when the deformation behavior of these materials is evaluated. Steady increase in the yield strength due to increasing strain rate was found for all studied grades, but the plastic deformation behavior of the grades differed clearly from each other. Increasing strain rate decreases the ductility of the stable EN 1.4301-2B grade while its strain hardening behavior remains relatively unchanged. The ductility of the unstable EN 1.4318-2B grade is less affected by the strain rate, but the strain hardening capability of this grade is clearly reduced by increasing strain rate, which leads to a relatively strong and, at low strain rates, negative dependence of the ultimate tensile strength on strain rate. Tests made at different temperatures for the EN 1.4318-2H/C850 grade show that decreasing test temperature increases the effect of strain rate on UTS. Martensite content measurements made on the specimens deformed to fracture show that both increasing strain rate and increasing test temperature reduce the total amount of strain-induced α'-martensite.

Acknowledgments

This work was supported by the Finnish Funding Agency for Technology and Innovation (Tekes) under Grant No. 40018/06 (Dypros/NewPro).

References

[1] S.S. Hecker, M.G. Stout, K.P. Staudhammer, J.L. Smith: "Effects of Strain State and Strain Rate on Deformation-Induced Transformation in 304 Stainless Steel: Part I. Magnetic Measurements and Mechanical Behavior", Metallurgical transactions. A, Physical metallurgy and materials science, 13 A, 1982, pp. 619-626

[2] J. Talonen: Effect of strain-induced α'-martensite transformation on mechanical properties of metastable austenitic stainless steels, Doctoral thesis, Helsinki University of Technology, 2007

[3] G.L. Huang, D.K. Matlock, G. Krauss: "Martensite formation, strain rate sensitivity, and deformation behavior of type 304 stainless steel sheet", Metallurgical transactions. A, Physical metallurgy and materials science, 20 A, 1989, pp. 1239-1246

[4] W.-S. Lee, C.-F. Lin: "Impact properties and microstructure evolution of 304L stainless steel", Materials Science and Engineering A, 308, 2001, pp. 124-135

[5] P. Larour, P. Verleysen, W. Bleck: Influence of uniaxial, biaxial and plane strain pre-straining on the dynamic tensile properties of high strength sheet steels, Journal De Physique. IV: JP, 134, 2006, pp. 1085-1090

[6] J. Talonen, P. Aspegren, H. Hänninen: "Comparison of different methods for measuring strain induced α′-martensite content in austenitic steels", Materials Science and Technology, 20, 2004, pp. 1506-1512

[7] M. Hokka, S. Curtze, V.-T. Kuokkala: Tensile HSB Testing of Sheet Steels at Different Temperatures, SEM Annual Conference & Exposition on Experimental and Applied Mechanics, Springfield, Massachusetts, USA, June 4-6, 2007

[8] S. Curtze, M. Hokka, V.-T. Kuokkala, T. Vuoristo: Experimental Analysis of the Influence of Specimen Geometry on the Tensile Hopkinson Split Bar Test Results of Sheet Steels, Materials Science and Technology (MS&T '06), Materials and Systems - Volume 2, Cincinnati, OH, USA, 2006, pp. 29-41

MICROSTRUCTURE EVOLUTION IN NANO/SUB-MICRON GRAINED AISI 301 STAINLESS STEEL

S. Rajasekhara[1], P.J. Ferreira[1], L.P. Karjalainen[2], A. Kyröläinen[3]

[1]The University of Texas at Austin, USA, [2]The University of Oulu, Finland, [3]Outokumpu Stainless Oy, Finland

Abstract

Transmission electron microscopy (TEM) has been used to analyze phase and microstructure evolution in a commercial metastable austenitic stainless steel – AISI 301, which has been cold-rolled to 52% reduction and subsequently annealed at 600°C, 800°C, and 1000°C, for short annealing times (1, 10 and 100 seconds). These studies reveal that the 52% cold-rolled AISI 301 stainless steel primarily consists of martensite microstructure. Annealing these cold-rolled samples at 600°C for short durations (1 and 10 seconds) results in negligible martensite to austenite reversion. However, the X-Ray diffraction data from samples annealed at a higher temperature of 800°C suggests austenite reversion and $M_{23}C_6$ carbide precipitation in these samples, which is confirmed by TEM images. Carbide precipitation is also observed in the images of samples annealed at 1000°C. Since carbide precipitation typically occurs in carbon containing stainless steels that are annealed for long durations (>0.1 hours/360 seconds) we report for the first time, carbide precipitation in a short annealed (1, 10 and 100 seconds), commercial austentitic stainless steel.

Keywords: Stainless Steel, Austenite, Stacking faults, Chromium carbide precipitation

Introduction

The roadmap for the next twenty-five years of the automotive industry, as laid out by the European Steel Technology Platform [1] is to develop Fe-based alloys that have exceptional strength and ductility. Stainless steels (SS) are good candidates due to their excellent corrosion resistance properties, but they lack the combination of high strength and ductility [2, 3]. This limitation may be overcome by developing an alloy with ultra-fine grains, which was first demonstrated in non-commercial metastable austenitic SS by Tomimura *et al.* [4] and Takaki *et al.* [5], and later by di Schino *et al.*[6, 7] and Ma *et al.* [8]. In these works, a metastable austenitic SS was heavily cold-rolled to produce deformation induced martensite (α'), and subsequently annealed to achieve ultra-fine grained austenite. More recently, our research group has applied this concept on commercial metastable austenitic AISI 301LN SS, where an enhancement of the mechanical properties was demonstrated [10-15]. Research has also been carried out on metastable austenitic AISI 301 SS, [10-13, 15, 16]. However this work was limited to microstructure analysis for samples annealed for long durations of time (30 min) [9]. In this work, the microstructure evolution of a heavily cold-rolled and short-annealed (< 100 seconds) AISI 301 SS is studied through transmission electron microscope analysis.

Experimental

Materials

An AISI 301 SS sheet with the composition shown in Table 1 was prepared by Outokumpu Stainless Oy, Tornio Works, Finland. The M_{d30} value, that indicates the temperature at which for a 30% true strain, 50% austenite to martensite transformation can be achieved, and the M_s value, which is the maximum temperature at which thermally induced martensite can form for this material, were calculated to be 32°C and -86°C, respectively [16]. The M_{d30} value above room temperature indicates that stress-induced martensite will form in samples deformed at ambient temperature. Samples from a 1.5 mm thick sheet were then subjected to 52% cold-reduction in a laboratory rolling mill at Outokumpu Stainless Oy.

Table 1. Chemical composition (in wt %) of AISI 301 SS used for this work.

	C	N	Ni	Cr	Mn	Si	Cu	Mo
301	0.10	0.07	6.3	16.7	1.18	1.06	0.24	0.65

Characterization

After cold rolling, the samples were annealed on a Gleeble 1500 thermo-mechanical simulator at the University of Oulu, Finland. The samples were heated at a rate of 200°C/sec and held at 600°C, 800°C or 1000°C for 1, 10 or 100 seconds. Subsequently, the samples were forced-air-cooled at a cooling-rate of approximately 200°C/s. Annealed specimens with dimensions ~ 85×10 mm^2, with a heated zone of 15 x 10 mm^2, were used for microstructure analysis by transmission electron microscopy.

Results and Discussion

Images of samples annealed at 600°C for different annealing durations are shown in Figure 1. Samples annealed for 1 second at this temperature (Figure 1a) show, primarily, a dislocation-cell type martensitic microstructure. Diffraction pattern analysis confirms this finding, where rings due to ultra-fine martensite phase are observed (Figure 1b). Streaks (for instance, (200)γ) corresponding to the austenite phase are also observed, which may be due to presence of retained austenite in the cold rolled sample. There is negligible difference between the images and diffraction patterns obtained from samples annealed for 1 and 10 seconds (Figs. 1a-d). The 10-second annealed sample has also substantial regions of dislocation-cell martensite and shows negligible martensite to austenite reversion. However, the TEM image of samples annealed at 600°C for 100 seconds, shown in Figure 1e, is substantially different from the 1-second and 10-second annealed samples. Austenite grains with high-angle grain boundaries can be clearly seen and confirmed by the corresponding diffraction pattern (Figure 1f). Stacking faults and secondary phase precipitates are also observed. Stacking faults are possible due to the low stacking fault energy of AISI 301 SS [17]. The secondary phase precipitates are likely to be $M_{23}C_6$ carbide precipitates as discussed by Padilha *et al.* [18, 19] and Weiss [20]. Not much can be said about whether the $\alpha' \rightarrow \gamma$ reversion follows a shear-type or diffusion type mechanism from the analysis of 600°C-annealed samples. Images of samples annealed at 800°C for different annealing durations are shown in Figure 2. Lath-type austenite with many defects is seen in samples annealed at 800°C for 1 second (Figure 2a), which is confirmed by the spot-like austenite diffraction pattern (Figure 2b). This is a clear indication of a shear-type $\alpha' \rightarrow$

γ reversion mechanism. The shear-type reversion mechanism in AISI 301 SS has also been reported by Somani *et al.* [10, 12, 15].

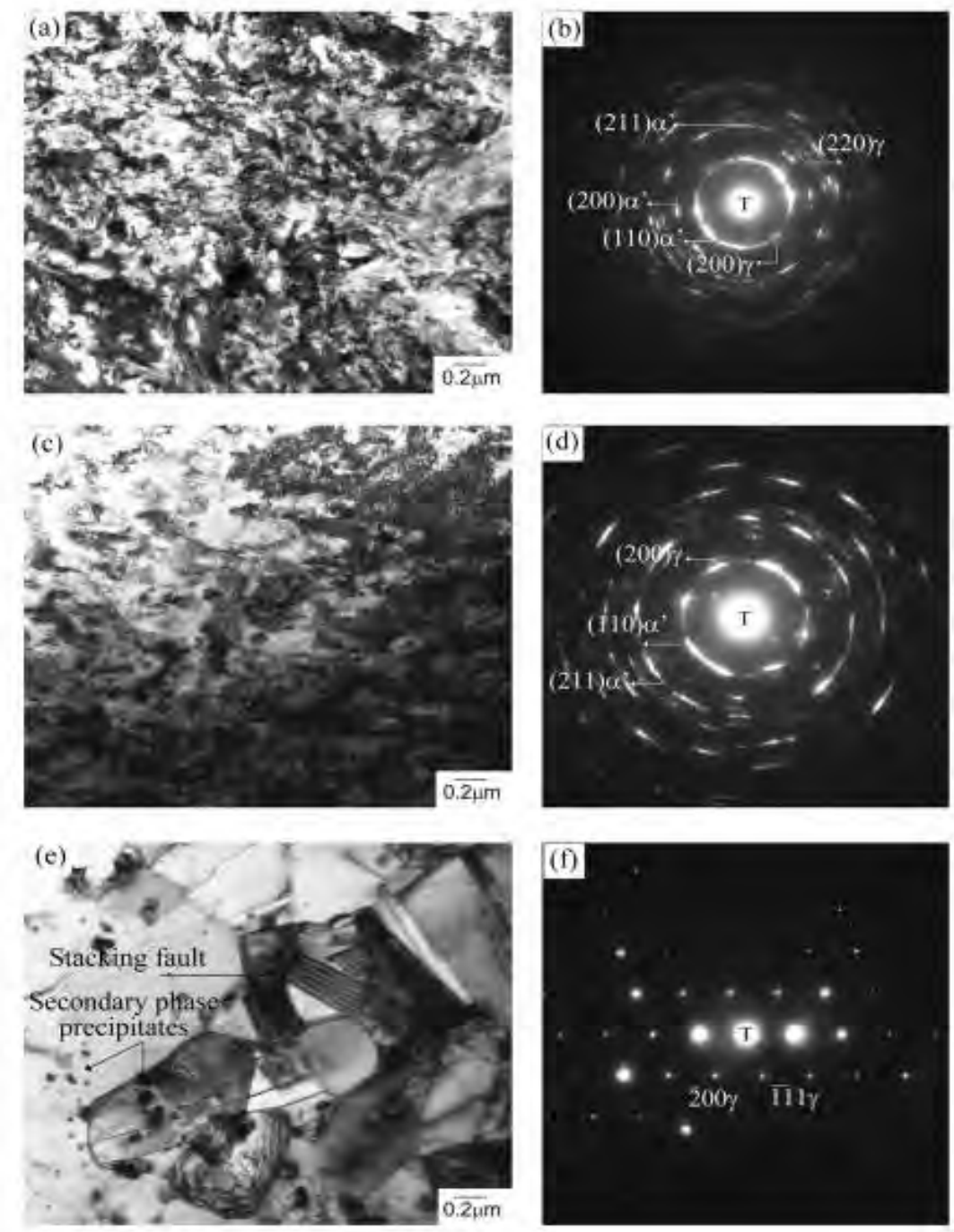

Figure 1. Annealing temperature of 600°C: (a), (c) and (e) are images for 1, 10 and 100 seconds respectively; (b), (d) and (f) are the corresponding diffraction patterns.

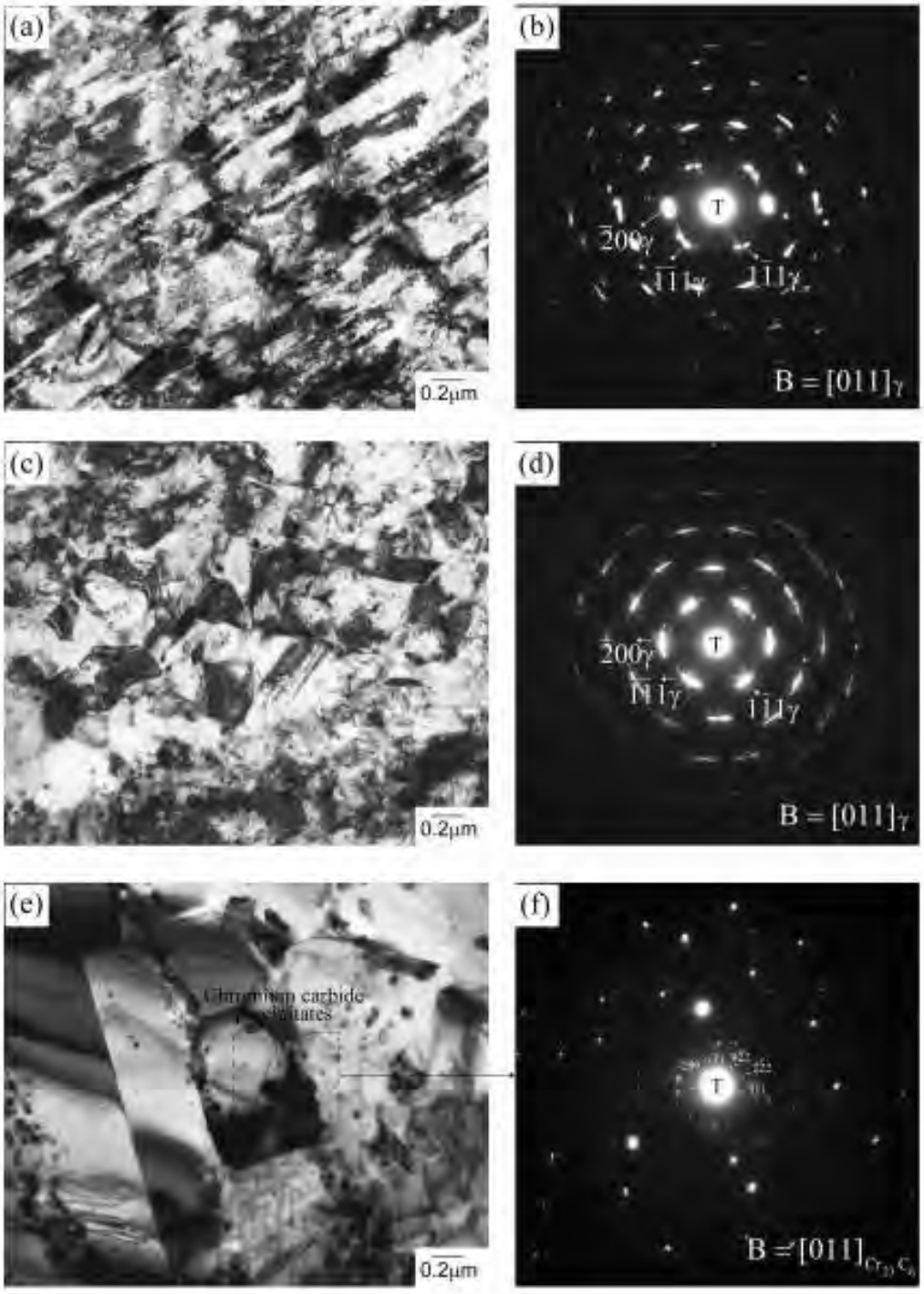

Figure 2. Annealing temperature of 800°C: (a), (c) and (e) are images for 1, 10 and 100 seconds respectively; (b), (d) and (f) are the corresponding diffraction patterns.

Samples annealed for a longer duration of 10 seconds exhibit similar microstructure (Figure 2c). However, annealing for longer durations result in grain growth and the lath-type austenite seen in Figure 2a is replaced by relatively defect-free austenite grains with high-angle grain boundaries. Stacking faults and carbide precipitation are also observed. These features (high angle grain boundaries, stacking faults and carbide precipitation) become more pronounced at longer annealing

duration of 100 seconds (Figure 2e). Carbide precipitations that grow to a size of ~ 0.1μm, are observed on grain boundaries,. These carbides can be clearly identified from their diffraction pattern (Figure 2f).

TEM images for the samples annealed at 1000°C are shown in Figure 3. Samples annealed for 1 second show large austenite grains with high-angle grain boundaries, as well as the formation of micro-twins (Figures 3a, 3b). Occurrence of micro-twins has been previously reported by Breedis in a Fe-Cr-Ni alloy [21]. Samples annealed for longer durations exhibit stacking faults and carbide precipitation. In these samples, the austenite grain size is larger and defect-free when compared with the 800°C-annealed samples, which may be attributed to grain growth at higher annealing temperature. Furthermore, there is a decrease in the number of secondary phase precipitates. Stacking faults were seen in samples that were annealed for 100 seconds at 600°C, 10 seconds and longer at 800°C, and for 1 second or longer at 1000°C (Figs. 1e, 2c, 2e, 3a-d). These faults may have originated during the diffusionless martensite to austenite transformation during the rapid annealing treatment of 1 second, and during the further re-arrangement of defect laden austenite upon annealing for longer durations of time. A detailed crystallographic analysis of stacking fault formation in these rapidly annealed AISI 301 SS would be interesting and may be addressed in the future. Carbide precipitation is also observed in these samples. This is an important observation because $Cr_{23}C_6$ at short annealing duration of 1 second (1000°C-anneal, Figure 3a) and at an annealing duration of 10 seconds (800°C-anneal, Figure 2c) have not been reported prior to this work.

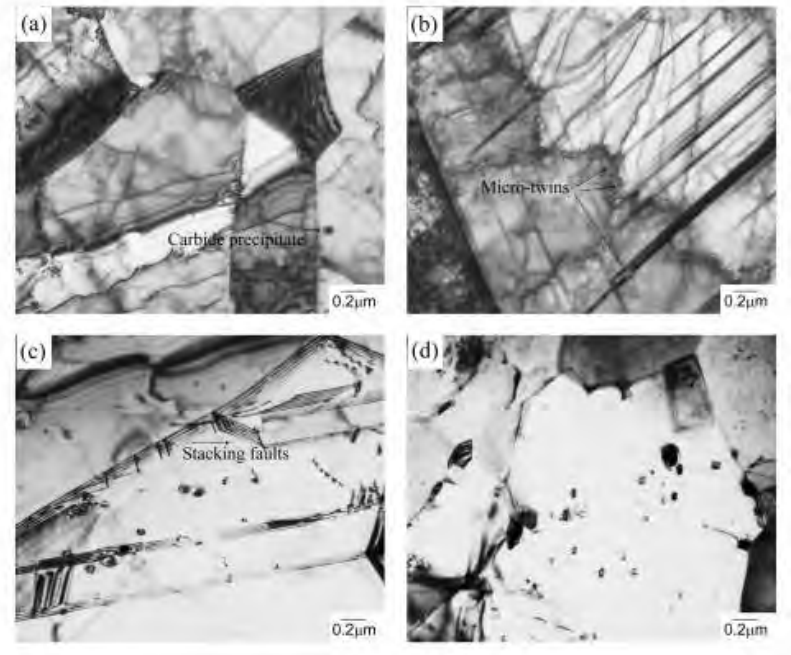

Figure 3. Annealing temperature of 1000°C: (a) Austenite grains in samples annealed for 1 second, (b) Micro-twins within large austenite grains in samples annealed for 1 second, (c) Stacking faults and carbide precipitation in samples annealed for 10 seconds, (d) carbide precipitation in samples annealed for 100 seconds.

Conclusions

In summary, this investigation has been conducted to understand the microstructure of 52% cold rolled and annealed AISI 301 stainless steel. The following conclusions can be drawn:

- Annealing the cold-rolled AISI 301 SS at a temperature of 600°C results in negligible austenite formation for annealing durations of 1 and 10 seconds. For the same annealing temperature, longer annealing durations (t >10 seconds) result in the formation of high-angle grain boundary austenite grains, stacking faults and secondary phase chromium carbides that are ~ 50nm in size.
- A shear type $\alpha' \rightarrow \gamma$ reversion mechanism is clearly observable when cold-rolled AISI 301 SS is annealed at 800°C for 1 second. Lath-type austenite grains with many defects are seen. At longer annealing durations, these lath-type austenite grains transform to grains with high angle boundaries. Stacking faults and large carbide precipitates are also observed.
- Samples annealed at 1000°C also have austenite grains with high-angle boundaries and stacking faults. There is a reduction in the concentration of carbides.

References

[1] 'European steel technology platform, Strategic research agenda; A vision for the future of the steel sector', *ESTEP – Belgium,* December 2005

[2] I.M. Bernstein, F.B. Pickner, *'Handbook of Stainless Steels'* 1st ed., New York, McGraw Hill (1977)

[3] The Materials Information Society. ASM Specialty Handbook: Stainless Steel. Metals Park: ASM International, 1994

[4] K. Tomimura, S. Takaki, S. Tanimoto, Y. Tokunaga, *ISIJ International,* 31 No. 7 (1991): 721-727

[5] S. Takaki, K. Tomimura, S. Ueda, *ISIJ International*, 34 No. 6 (1994): 522-527

[6] A. di Schino, I. Salvatori, J.M. Kenny, *J. Mater. Sci. Lett.,* 21 (2002): 751-753

[7] A. di Schino, M. Barteri, J.M. Kenny, *J. Mater. Sci.*, 38 (2003): 4725-4733

[8] Y. Ma, J. E. Jin, Y. K. Lee, *Scripta Mater.,* 52 (2005): 1311

[9] D.L. Johannsen, P.J. Ferreira , A. Kyröläinen, *Metall. Trans. A*, 37 (2006): 2325-2338

[10] M.C. Somani, L.P. Karjalainen, P. Juntunen, S. Rajasekhara, P.J. Ferreira, A. Kyröläinen, T. Taulavuori, P. Aspegren, *International Symposium on Ultrafine Grained Steels -2005, Sanya, China. Proceedings published in Iron & Steel,* 40 (2005): 232

[11] S. Rajasekhara, M.C. Somani, L.P. Karjalainen, A. Kyröläinen, P.J. Ferreira, *International Symposium on Ultrafine Grained Steels – 2005, Sanya, China. Proceedings published in Iron & Steel,* 40 (2005): 283

[12] M.C. Somani, L.P. Karjalainen, A. Kyröläinen, T. Taulavuori, P. Aspegren, *Proc. of the 5th European Steel Congress, Science & Market, Seville, Spain,* September (2005): 37

[13] S. Rajasekhara, M.C. Somani, M. Koljonen, L.P. Karjalainen, A. Kyröläinen, P.J. Ferreira, *MRS Fall Meeting– 2005, Boston, MA, USA*

[14] S. Rajasekhara, P.J. Ferreira, L.P. Karjalainen, A. Kyröläinen, *Metall. Trans. A*, 38 (2007): 1202-1210

[15] M.C. Somani, L.P. Karjalainen, A. Kyröläinen, T. Taulavuori, *Mater. Sci. Forum,* 539-543 (2007): 4875-4880

[16] T. Sourmail, *Mater. Sci. Tech.,* 17 (2001): 1-14

[17] P.J. Ferreira, P. Muellner, *Acta Mater.*, 46 (1998): 4479

[18] A.F. Padilha, R.L. Plaut, P.R. Rios, *ISIJ International*, 43 (2003): 135-143

[19] A.F. Padilha, P.R. Rios, *ISIJ International*, 42 (2002): 325-337

[20] B. Weiss, R. Stickler, *Metall. Trans.*, 23A (1992): 2455-2467

[21] J.F. Breedis, *Trans. Am. Inst. Metall. Engg.*, 236 (1966): 218-219.

KINETICS OF GRAIN GROWTH IN ULTRA-FINE GRAINED AISI 301LN STAINLESS STEEL

S. Rajasekhara[1], P.J. Ferreira[1], L.P. Karjalainen[2], A. Kyröläinen[3]

[1]The University of Texas at Austin, USA, [2]The University of Oulu, Finland, [3]Outokumpu Stainless Oy, Finland

Abstract

Ultra-fine grained austenite has been produced in a commercial AISI 301LN stainless steel (SS) by first cold rolling a sheet to 63% reduction and subsequently annealing at 800°C, 900°C and 1000°C for periods of time ranging from 1 second to 100 seconds. In the course of annealing, the deformation induced martensite, produced during cold rolling, is reverted to ultra-fine grained austenite. An average grain size is estimated for all annealed samples, which is used to calculate the kinetic grain growth parameters *k* and *n*. From the analysis of these parameters, we find that 1) ultra-fine grained AISI 301LN SS have a $\Delta G_{activation}$ value similar to conventional austenitic stainless steels (~ 205kJ/mol), 2) rapid grain growth occurs during the initial periods of annealing (1-100 seconds) due to the high curvature of grain boundaries and consequently large driving forces for grain growth, and 3) enhanced grain boundary mobility is responsible for extended grain growth at simulated long annealing durations (> 10 hours).

Introduction

The roadmap for the next twenty-five years of the automotive industry, as laid out in the European Steel Technology Platform [1] is to develop steels that have exceptional strength and ductility [2-6]. With these novel materials, engineers will be able to design structures that can withstand (withstand?) natural environments (such as humid air and corrosive media), are durable and light-weight. Stainless steels (SS) are good candidates for such applications due to their excellent corrosion resistance properties and good ductility, but they lack high strength. In that context, an interesting exercise is to use metastable austenitic SS grades with ultra-fine grains that possess the combination of high strength and ductility. Specifically, an interesting concept involves heavy cold-rolling of metastable austenitic SS to produce deformation induced martensite (α'), which reverts to ultra-fine grained austenite upon annealing [3-9]. In this fashion, ultra-fine grains contribute significantly to the overall yield strength through grain boundary strengthening. Prior research has focused mainly on non-commercial specialty metastable alloys [4-6]. More recently, this concept has been applied to a commercial metastable austenitic SS, AISI 301LN SS, where enhanced mechanical properties were demonstrated [10-15]. Although this development is promising from a commercial perspective, an understanding of the microstructural evolution, the kinetics of ultra-fine grain growth and the kinetics of $\alpha' \rightarrow \gamma$ reversion is required. While research on the microstructural evolution has been addressed in detail through both optical and transmission electron microscopy [10-13, 15, 16], the kinetics of grain growth has not been investigated. In the work discussed herein,

the kinetics of ultra-fine grain growth is analyzed. In particular, the activation energy, driving force for grain growth and grain boundary mobility are determined and discussed.

Experimental

AISI 301LN stainless steel samples with the composition shown in Table 1 were prepared by Outokumpu Stainless Oy, Tornio, Finland. The M_{d30} and M_s values for this material were calculated to be 35°C and -127°C, respectively [17].

Table 1. Chemical composition (in wt %) of AISI 301LN SS used in this work.

	C	N	Ni	Cr	Mn	Si	Cu	Mo
301LN	0.017	0.15	6.5	17.3	1.29	0.52	0.2	0.15

The M_{d30} value above room temperature enables the formation of strain induced martensite in samples deformed at ambient temperature. As-cast samples were hot-rolled and then subjected to cold-rolling (63% reduction) at Outokumpu Stainless Oy, Tornio, Finland. Next, 0.4 mm thick strips were annealed in a Gleeble-1500 thermo-mechanical simulator at the University of Oulu, Finland. The samples were heated at the rate of 200°C/s and held at 800°C, 900°C and 1000°C for 1, 10 and 100 seconds, respectively. Subsequently, the samples were forced-air-cooled at a cooling-rate of approximately 200°C/s. Samples were then used for TEM studies, performed on a JEOL 200CX and a 2010F electron microscope operating at 200kV. To estimate the average grain sizes, measurements were taken along the longest grain direction and perpendicularly, and from these two values the mean was calculated for each grain. A statistically significant sample-size of 100 grains from each of the annealed samples was measured to obtain the average grain size $\bar{\mathbf{d}}$ for a particular sample.

Results

The average grain sizes for all annealing treatments are shown in Figure 1. A large difference in grain sizes obtained for the various annealing conditions can be observed. For instance, samples annealed at 800°C exhibit a rapid grain growth from ~ 0.5μm to ~ 2.4μm when the annealing duration is increased from 1 to 100 seconds, while the samples annealed at 900°C and 1000°C show a dramatic grain growth with the average grain sizes increasing from 1.2μm to 6.1μm, and 1.5μm to 10.1μm, respectively. Such a rapid grain growth in samples annealed at higher temperatures has not been reported earlier. Understanding the reason for this behavior is crucial to develop and sustain ultra-fine grains in SS. In this regard, the kinetics of grain growth in AISI 301LN SS is investigated in this work.

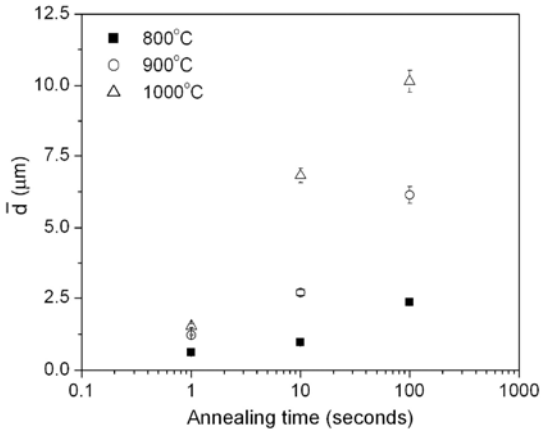

Figure 1. Grain size calculations for AISI 301LN SS samples; annealed at 800°C, 900°C and 1000°C.

Discussion

Kinetics of ultra-fine grain growth

The kinetics of nano/sub-micron grain formation may be evaluated by analyzing the generalized grain growth law, which is expressed by [18-25]:

$$\left(\bar{\mathbf{d}} - \bar{\mathbf{d}}_{\mathbf{o}}\right)^{n} = kt, \tag{1}$$

where $\bar{\mathbf{d}}$ is the average austenite grain size, $\bar{\mathbf{d}}_{\mathbf{o}}$ the initial austenite grain size, n the grain growth exponent, k the grain growth parameter and t the annealing time. The grain growth kinetic parameters, k and n, were estimated by regression analysis of the average grain size data $\bar{\mathbf{d}}$ obtained for samples annealed at 800°C, 900°C and 1000°C, according to equation(1).

The initial austenite grain size $\bar{\mathbf{d}}_{\mathbf{o}}$ was assumed to be the average grain size (0.1μm) of samples annealed at 600°C for 1 second because, as discussed elsewhere [15, 16], this was the annealing condition where the first martensite to austenite reversion could be observed.

A modified form of equation (1) suitable for regression analysis can be written as follows:

$$\ln\left(\bar{\mathbf{d}} - \bar{\mathbf{d}}_{\mathbf{o}}\right) = \frac{1}{n}\ln(k) + \frac{1}{n}\ln(t), \tag{2}$$

where the symbols have the same meaning as before. Values of the grain growth exponent - n, obtained from the regression of equation (2) are shown as a function of annealing temperature (Figure 2a). A value of $n = 2$ is expected for an ideal material with no impurities, near the melting temperature, and spherical grains [20, 21, 23]. However, for real materials the grain growth exponent is typically greater than 2. This is because 1) grains are not spherical and 2) there are inclusions or chemical segregation at the grain boundaries that inhibit grain growth [20]. In the context of ferrous alloys, Mizera *et al.* have experimentally estimated the grain growth exponent for AISI 316L samples annealed at 1050°C to be ~ 2.77 [26]. Here, AISI 301LN SS used in this work

exhibits a value of $n \sim 2.36$ for a similar annealing temperature (1000°C). This difference is likely due to a difference in alloy composition.

A regression analysis of equation (2) also yields the values of the kinetic parameter *k* as a function of annealing temperature (Figure 2b). It is observed that value of the grain growth constant *k* increases as the annealing temperature increases. As will be discussed in a later section, this behavior may be attributed to an increased mobility of atoms taking part in the grain growth process, a characteristic that has an exponential dependence with annealing temperature.

Knowing the kinetic parameter *k*, the activation energy for grain growth can be estimated from this relationship [27]:

$$k = k_o \exp\left(-\frac{\Delta G_{activation}}{RT}\right), \tag{3}$$

where k_o is a material constant, $\Delta G_{activation}$ the activation energy for grain growth, *R* the gas constant, and *T* the annealing temperature.

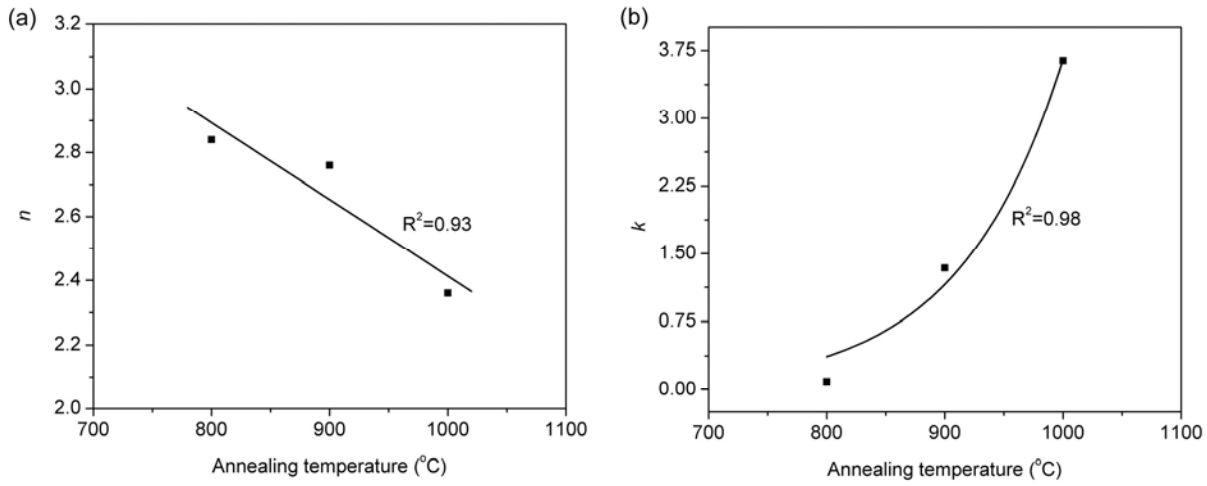

Figure 2. Estimation of the kinetic parameters, (a) grain growth exponent – *n*, (b) grain growth constant - *k*. The calculation is based on a regression analysis of equation (2) for samples annealed at 800°C, 900°C and 1000°C.

Linear regression analysis carried out on equation (3) yields $k_o \approx 2.69 \times 10^9\, m.\sec^{-1}$, from which $\Delta G_{activation} \sim$ 205kJ/mol (Figure3). The activation energy values are close to values reported for several conventional stainless steels (AISI 304, 316, 321 and 347) [28-32].

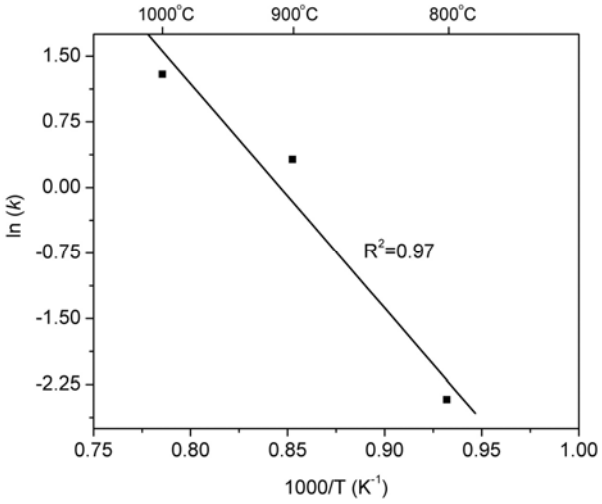

Figure 3. Determination of the $\Delta G_{activation}$ and the parameter k_0.

In his work, German [28] plotted the $\Delta G_{activation}$ as a function of the grain growth exponent, *n*, for various conventional SS. As the AISI 301LN SS yielded an average value of $n \sim 2.6$, the $\Delta G_{activation}$ values for various conventional SS have been taken from the work of German for $n \sim 2.6$ for comparison.. It was found that the activation energy for AISI 301LN SS is close to those of AISI 304 and 316 SS. On the other hand, the activation energies of AISI 321 SS and 347 SS are much higher than those of AISI 301LN, 304 and 316 SS. This is because AISI 321 and 347 SS have titanium (Ti) and columbium (niobium). The official chemical symbol is: (Nb) additions respectively, which form stable carbides (TiC, NbC) [29, 30]. These create back-stress on grain boundaries hindering their motion, thereby raising the activation energy for grain growth [20].

Knowing the kinetic parameters (*k*, *n*) and $\Delta G_{activation}$, grain size in AISI 301LN SS can be estimated as a function of annealing conditions. As seen from Figure 4a, rapid grain growth is predicted at short annealing durations for all annealing temperatures. This may be due to a large grain growth driving force associated with high curvature of nano/sub-micron grains formed after $\alpha' \rightarrow \gamma$ reversion. However, interesting differences arise at longer annealing durations. For instance, at a low annealing temperature of 800°C, on the basis of calculation, it seems that the grain size would converge to
~ 20μm after an annealing duration of 10 hours whereas at a higher annealing temperature of
~ 1000°C significant grain growth is still possible after 10 hours of annealing.

This result may be explained if grain boundary mobility is also considered (Figure 4b). Since grain boundary mobility (*M*) is related to *k* and $\Delta G_{activation}$ as $M = C\exp\left(\frac{\Delta G_{activation}}{RT}\right)$ where *C* is a constant [34], its value increases exponentially when annealing temperature is raised from 800°C to 1000°C resulting in larger grain sizes at higher annealing temperatures.

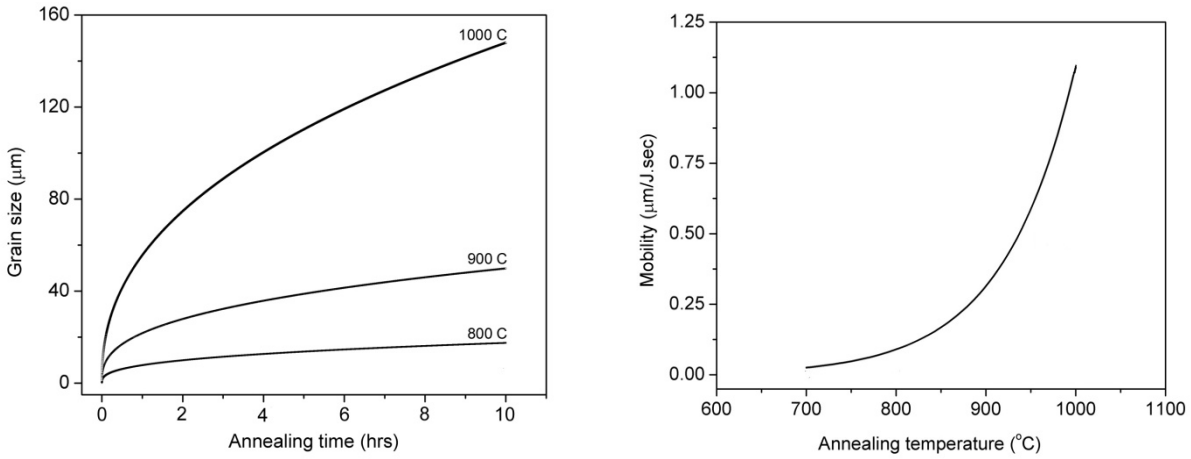

Figure 4. (a) Calculated grain growth curves as a function of annealing conditions (*t*, *T*), (b) Grain boundary mobility as a function of annealing temperature in AISI 301LN SS.

Conclusions

The TEM analysis of annealed samples reveals the presence of ultra-fine austenite grains that rapidly grow in size. The reasons for rapid grain growth were determined by analysis of the kinetic parameters, activation energy ($\Delta G_{activation}$) and driving force (ΔG) for grain growth. The analysis shows that the $\Delta G_{activation}$ for AISI 301LN is similar to that of other SS and may not satisfactorily explain the observed fast grain growth rates in AISI 301LN SS. However, a generalized expression for ΔG, which depends on experimental conditions as well as kinetic parameters, can offer two explanations for this: 1) ultra-fine grains formed during short annealing treatments exhibit a large driving force for grain growth, and 2) high annealing temperatures increase grain boundary mobility, which promotes grain growth.

References

[1] 'European steel technology platform, Strategic research agenda; A vision for the future of the steel sector', *European Commission, Belgium,* December 2005

[2] Steel grades, properties and global standards, Outokumpu Stainless Oy.

[3] Y. Ma, J. –E. Jin, Y. –K. Lee, *Scripta Mater.,* 52 (2005): 1311-1315

[4] K.Tomimura, S. Takaki, S. Tanimoto, Y. Tokunaga, *ISIJ International* 31 (1991): 721-727

[5] K. Tomimura, S. Takaki, Y. Tokunaga, *ISIJ International* 31 (1991): 1431-1437

[6] S. Takaki, K. Tomimura, S. Ueda, *ISIJ International* 34 (1994): 522-527

[7] A. di Schino, M. Barteri, J. M. Kenny, *J. Mater. Sci. Lett.*, 21 (2002): 751-753

[8] A. di Schino, M. Barteri, J. M. Kenny, *J. Mater. Sci.,* 38 (2003): 4725- 4733

[9] A. di Schino, J. M. Kenny, M. G. Mecozzi, M. Barteri, *J. Mater. Sci.,* 35 (2000): 4803-4808

[10] M. C. Somani, L. P. Karjalainen, M. Koljonen, P. Aspegren, T. Taulavuori, A. Kyröläinen, *Proc. 5th European Cong. Stainless Steel, Science and Market*, September (2005): 37-42

[11] M. C. Somani, L. P. Karjalainen, A. Kyröläinen, T. Taulavuori, *Mater. Sci. Forum* 539-543 (2007): 4875-4880

[12] M. C. Somani, L. P. Karjalainen, P. Juntunen, S. Rajasekhara, P. J. Ferreira, A. Kyröläinen, *International Symposium on Ultra-fine Grained Steels, September 2005, Sanya, China*

[13] P. Juntunen, M. C. Somani, L. P. Karjalainen, Kyröläinen, A., *International Symposium on Advanced Steels, April 2007, Chennai, India*

[14] D. L. Ritterman, A. Kyröläinen, P. J. Ferreira, *Metall. Trans.*, 37A (2006): 2325-2338
[15] S. Rajasekhara, L. P. Karjalainen, A. Kyröläinen, P. J. Ferreira, (submitted)
[16] S. Rajasekhara, *Development of nano/sub-micron grain structures in metastable austenitic stainless steels*, The University of Texas – Austin, Doctoral dissertation, (2007): pp 110
[17] T. Sourmail, *Mater. Sci. Tech.*, 17 (2001): 1
[18] G. Gottstein, L. S. Shvindlerman, *Grain Boundary Migration in Metals*, 1st Ed., Boca Raton, CRC Press (1999)
[19] P. Feltham, *Acta Metall.*, 5 (1957): 97-105
[20] M. Hillert, *Acta Metall.*13 (1965): 227
[21] G. T. Higgins, *Met. Sci.*, 9 (1974): 143-150
[22] N. P. Louat, *Acta Metall.*, 22 (1974): 721-724
[23] H. Hu, B. B. Rath, *Metall. Trans.*, 1A (1970): 3182-3184
[24] H. V. Atkinson, *Acta Metall.*, 36 (1988): 469-491
[25] H. Fredriksson, *Mater. Sci. Tech.*, 6 (1990): 811-817
[26] J. Mizera, J. W. Wyrzykowski, K. J. Kurzydlowski, *Mater. Sci. Engg. A*, 104 (1988): 157-162
[27] D. A. Porter, K. E. Easterling, *Phase Transformations in Metals and Alloys*, 1st Ed., London, Chapman & Hall (1990)
[28] R. M. German, 'Grain growth in austenitic stainless steels', *Metallography*, 11 (1978): 235-239
[29] J. E. Spruiell, J. A. Scott, C. S. Ary, Hardin, *Metall. Trans.*, 4A (1973): 1533-1544
[30] A. S. Grot, J. E. Spruiell, *Metall. Trans.*, 6A (1975): 2023-2030
[31] J. K. Stanley, A. J. Perotta, *Metallography*, 2 (1969): 349
[32] W. Przetakiewicz, K. J. Kurdlowski, M. W. Grabski, *Mater. Sci. Tech.*, 2 (1986): 106-109

REVERSION TRANSFORMATION OF COLD ROLLED MARTENSITE TO AUSTENITE IN EN 1.4318 METASTABLE AUSTENITIC STEEL: MICROSTRUCTURES AND MECHANISMS

M.C. Somani[1], L.P. Karjalainen[1], R.D.K. Misra[2], P. Juntunen[1], A. Kyröläinen[3]

[1]University of Oulu, Finland, [2]University of Louisiana at Lafayette, USA, [3]Raahe Region Technology Center Ltd, Finland

Abstract

The ingenious concept of creating submicron grained microstructures in a commercial 17Cr-7Ni austenitic stainless steel type EN 1.4318 (AISI 301LN) by reverting strain-induced martensite to ultra-fine austenite has been applied to examine the transformation characteristics and mechanisms. The microstructural features of the ultra-fine grains observed in TEM in the domain of optimized processing conditions are briefly illustrated. The influence of prior cold rolling reduction on the formation of ultra-fine reverted austenite grains is clearly established. Other mechanisms operating during cold rolling and subsequent annealing are highlighted in this paper.

Introduction

An ever-increasing demand for improving the mechanical properties of austenitic stainless steels has led to the development of newer processing routes, cf.[1] This study forms a part of an extensive research programme to develop ultra-fine grained microstructures in metastable austenitic stainless steels by reversion annealing, e.g. for applications requiring high strength with good ductility and formability. Extensive investigations were carried out to examine the effects of chemical composition and cold rolling reduction on the reversion mechanisms and microstructures of metastable 17Cr-7Ni stainless steel types EN 1.4318 (AISI 301LN), EN 1.4310 (AISI 301), and some experimental heats.[2-5]

After reversion annealing in the temperature range 725-800°C for extremely short durations of 1-10 s, quite an exceptional combination of yield strength/elongation (700-1000 MPa/50-30%) could be achieved for EN 1.4318 steel, prior cold rolled to 45-76% reduction. Variation in microstructures was quite evident, as the reversion kinetics was found to be strongly dependent on the prior cold rolling reduction and annealing parameters. [2,3,5] In this paper, microstructural features of the ultra-fine grains observed in EN 1.4318 steel along with other features detected by transmission electron microscopy are briefly illustrated at the annealing temperatures of highest interest, viz., 730 and 800°C.

Experimental

An annealed strip of commercial EN 1.4318 steel, about 1.5 mm thick, having the following chemical composition (in wt.-%): 0.017C-0.52Si-1.3Mn-17.3Cr-6.5Ni-0.15Mo-0.15N, was cold rolled to 45% and 62% reduction in a laboratory rolling mill and subsequently annealed on a Gleeble 1500 thermomechanical simulator. For the annealing experiments, cold rolled strips of

dimensions 120 mm x 10 mm were subjected to annealing at 730 and 800°C for 1 or 10 s. The heating rate used was 200°C/s and the cooling rate was also around 200°C/s down to 400°C. Pieces of annealed specimens measuring 10 mm x 10 mm from the uniform hot zone in the centre of the specimens were used for TEM studies, performed on a Hitachi 7600 Scanning Transmission Electron microscope operated at 100 kV. Thin foils were prepared by twin-jet electropolishing 3 mm discs, punched from specimens ground to ~100 μm thickness, using a solution of 10% perchloric acid in acetic acid electrolyte.

Results and discussion

The details of strain induced martensitic transformation during cold rolling and the effects of cold rolling reduction on reversion annealing characteristics of EN 1.4318 and EN 1.4310 steels have been described in detail elsewhere, cf. [2,3] The characteristics of α'- γ reversion under the influence of processing parameters and the corresponding microstructural features and reverted austenite grain size are discussed in the following sections.

α'- γ reversion

The reversion phenomenon either by martensitic shear or diffusional transformation has been well illustrated in the literature for a number of Cr-Ni or austenitic stainless steels, cf. [6-8] Typical transformation kinetics as a function of annealing temperature for isochronal treatment (1-10 s holding) for EN 1.4318 steel cold rolled to different reductions (45, 60 and 76%) were suitably modelled in the form of Avrami type regression equations. [3,5] Recently, Rajasekhara[9] has modelled the transformation kinetics using the generalized Avrami relationship for diffusion controlled phase transformations, and assuming a time and temperature dependent grain growth rate and a time-independent but temperature dependent nucleation rate. A reasonable fitting was observed but with scarce data.

In experiments, the transformation rate was found to be dependent on annealing time and also strongly on the degree of prior cold reduction, [3,5] as reproduced in Figure 1, which shows that the reversion process is quite fast after 75% CR. Even without any holding at 700°C, there is extensive transformation (austenite fraction above 70%) and it gets nearly completed in about 6 s. However, at 45% CR, the kinetics are slower, so that there was still about 10% martensite in the microstructure after about 100 s. SQUID data for 62% CR steel taken from Rajasekhara[9] supports the data shown in Figure 1 well, even though the different measurement techniques can affect the results.

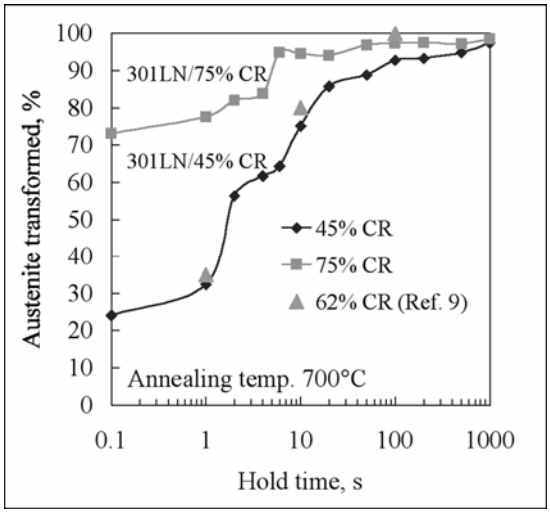

Figure 1. Effect of cold rolling reduction on the kientics of martensite to austenite reversion in EN 1.4318 as estimated by magnetic measurements. SQUID data obtained by Rajasekhara[9] on 62% CR specimens are included for comparison.

Microstructures of reversion-annealed EN 1.4318 stainless steel

Because the transformation for EN 1.4318 steel was essentially diffusion controlled, as also confirmed by X-ray diffraction and microstructural analysis,[3-5] the austenite formation occurs by nucleation and growth. Figure 2 shows typical TEM micrographs obtained following the reversion annealing at 730 and 800°C for 1 or 10 s, the optimimal reversion range, which gave excellent combinations of strength and ductility that exceed the values obtained in current industrial production of EN 1.4318 grade. [4,5] The following subsections describe briefly the microstructural features, the mechanisms operating in reversion and the formation of ultra-fine reverted austenite grain structure and its dependence on prior cold rolling reduction.

Characteristic structural features

Owing to its low stacking fault energy (SFE), fault bundles are readily formed in austenitic stainless steels in the course of cold deformation. The SFE of EN 1.4318 steel with similar nitrogen content (0.15%) has been experimentally estimated to be about 15 mJ/m^2. [10] On annealing at 730°C, stacking faults along with high dislocation densities can be seen in deformed austenite at both 45% CR and 62% CR (Figures 2a and 2b, respectively), but they are less frequently observed after annealing at higher temperature of 800°C.

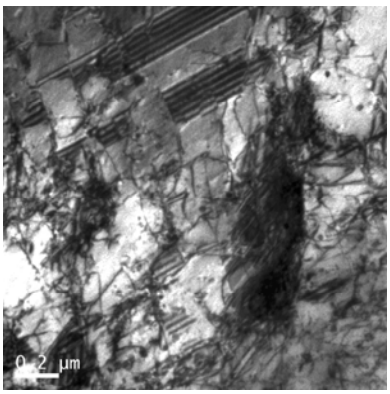

(a)

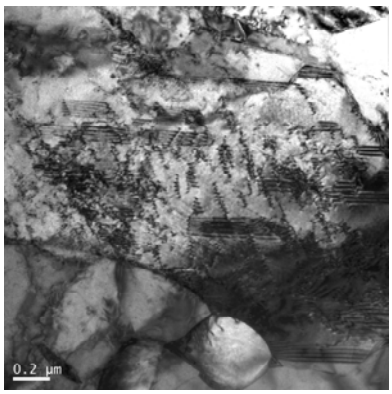

(b)

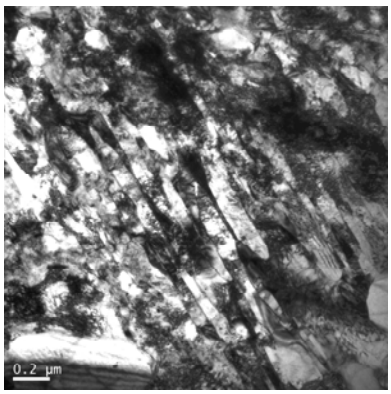

(c)

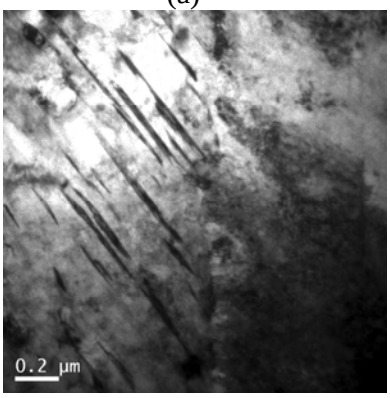

(d)

Figure 2. TEM micrographs of the cold rolled and reversion-annealed EN 1.4318 steel showing detailed microstructural features: (a) 730°C/10 s/ 45% CR, (b, c) 730°C/1 s/ 62% CR and (d) 730°C/1 s/ 45% CR.

On the other hand, martensite laths are frequently seen with or without reverted austenite grains along the laths in specimens annealed at 730°C, as shown in Figure 2c for a 62% CR specimen annealed for 1 s. From our regression equations based on X-ray diffraction data, [3,5] it is expected that there would be about 4% and 8% unreverted martensite fractions in the 62% and 45% CR specimens, respectively, following annealing at 730°C for 1 s, although the estimation of low fractions (< 5%) cannot be very accurate owing to the limitations imposed by the technique. SQUID data from Rajasekhara[9] indicated ~65% martensite left in the 62% CR steel after

annealing at 700°C for 1 s. However, raising the annealing temperature to 800°C practically transforms all martensite to austenite within a very short duration of 1 s, even though a few traces of martensite laths can still be seen in some areas.

Besides martensitic laths, commonly observed in specimens annealed at 730°C (Figure 2c), both twinned martensite and microtwins in deformed austenite were occasionally observed in 45% CR specimens annealed at 730°C. An example of microtwins is shown in Figure 2d. Formation of mechanical twins in austenitic stainless steels is due to regular overlapping of stacking faults in successive {111} planes[10] and are infrequently seen in faulted austenite.

Takaki et al. [8] has earlier described the diffusional nucleation-growth type reversion process in a 50% cold rolled Fe-18.08Cr-8.65Ni alloy (nearly fully transformed to martensite). They showed that, following annealing at 500°C for 90 min, the reverted austenite nucleated at lath boundaries in the form of thin plates that resulted in the formation of laths and blocks of austenite. Thus the reverted austenite inherited the morphological characteristics from lath-martensite even in a diffusional reversion, similarly as noticeable here in the 62% CR specimen annealed at 730°C for 1 s (Figure 2c). Further heavy prior cold working (90% CR) caused the destruction of lath martensitic structure, resulting in the formation of dislocation-cell structure and ultimately leading to fine equiaxed γ grains on reversion. [6,8] In consistence, two morphologies of austenites have been reported in the literature for an 18% Ni 350 grade maraging steel following reversion annealing. [11] The first, as usual, formed at the martensite lath boundaries and the other nucleated inside the martensite laths in the form of Widmanstatten plates. These Widmanstatten plates mostly appeared as coupled twins with a distinct midrib, which was found parallel to $\{111\}_\gamma$ and $\{110\}_\alpha$ planes.

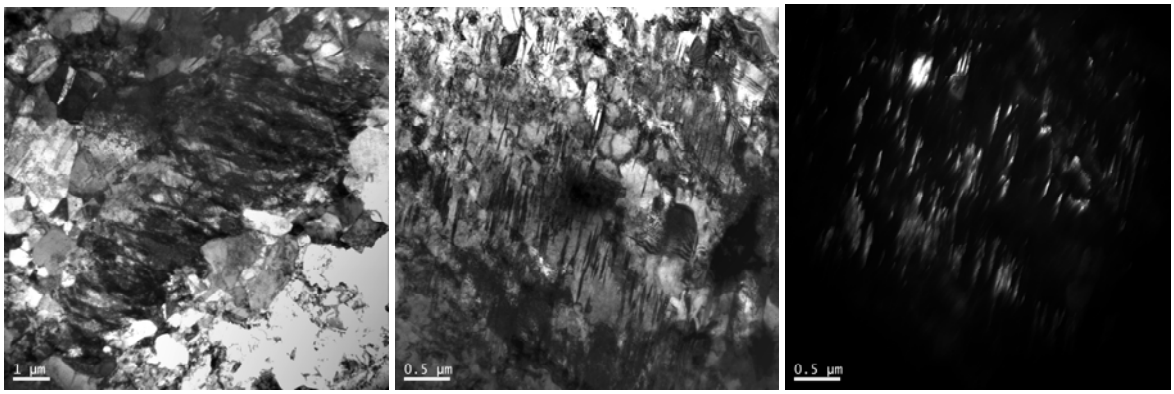

(a) (b) (c)

Figure 3. Reversion of martensite to austenite at (a) lath boundaries (800°C/1 s/ 62% CR) and (b) as intralath layers of reverted γ (730°C/1 s/45% Cr), as also confirmed by (c) dark field image.

Figure 3 shows the presence of fine equiaxed reverted austenite grains along with martensitic laths revealing the occurrence of nucleation and growth of austenite grains at marternsite lath boundaries. Hence, the observations here for EN 1.4318 steel are in accordance with those of Takaki et al. [8] The second type of austenite nucleation, where reverted intralath γ layers in the form of thin plate are present traversing the martensitic laths, can be seen in the 45% CR specimen annealed at 730°C for 1 s (Figure 3b). This is further confirmed by the dark field image showing the diffraction contrast from the intralath austenite layers (Figure 3c). The mechanism of the formation of these layers is not clearly understood. The features noticed in EN 1.4318 (Figure 3b), though noticeably similar as given in literature, [11] need further investigation.

Precipitation of carbides is commonplace in austenitic stainless steels, particularly at temperatures in the vicinity of 800°C. [12] Though seen frequently in some specimens, it was beyond the scope of this work to investigate the nature of these strain induced precipitates and more details are available in another contemporary paper presented in this conference. [13]

Grain size

The effect of cold rolling reduction on the reversion can be easily ascertained from the microstructures of specimens annealed at 730°C/1 s. A higher reduction (62%, Figure 4b) has led to the formation of a larger number of reverted γ nuclei and hence much finer transformed nano- to submicron austenite grains (0.2 μm) in comparison to that in 45% CR specimen (0.65 μm; Figure 4a).

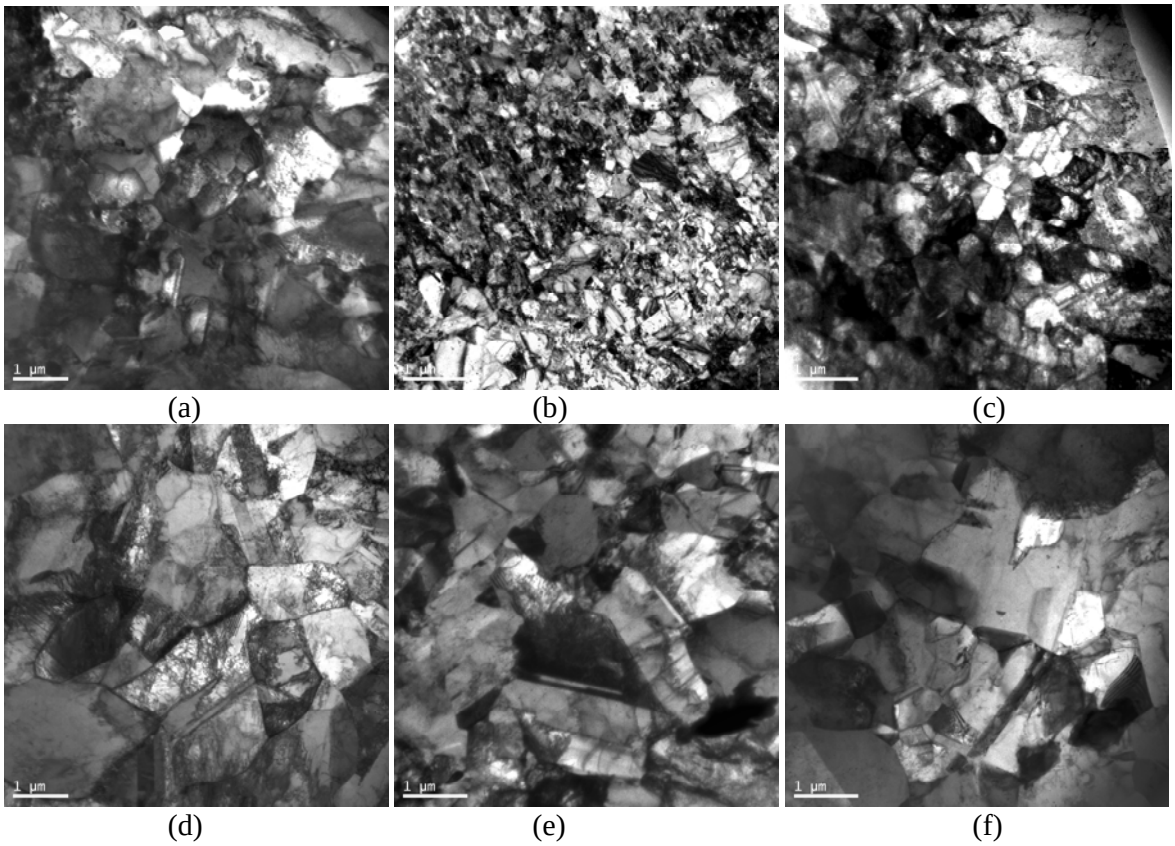

Figure 4. TEM micrographs of cold rolled and reversion-annealed EN 1.4318 steel showing reverted grain structures at different conditions: (a) 730°C/1 s/ 45% CR, (b) 730°C/1 s/ 62% CR, (c) 730°C/10 s/ 62% CR, (d) 800°C/10 s/ 45% CR, (e) 800°C/1 s/ 62% CR, and (f) 800°C/10 s/ 62% CR.

Also, the initial martensite fractions were quite different at the two reductions, about 62% and 82%, at 45% CR and 62% CR, respectively, [2,3,5] which suggests a possibility of achieving extremely fine, even nanoscale, grain structure at still higher reductions in a very short time of ≤1 s. These results are similar to those reported by Takaki et al. [8] Holding at 730°C for10 s, however, did not show any significant effect of holding time in the 45% CR specimen, but in the 62% CR specimen there was appreciable grain growth (0.53 μm; Figure 4c), where the reversed grain size was slightly finer than that of 45% CR specimen as annealed at 730°C/1 s (Figure 4a). Annealing at 800°C for 1 s has resulted in appreciable coarsening of grains and the grain size was not very different for the 45% and 62%CR specimens (1.1 and 0.8 μm, respectively; Figure 4d-e). Also α'- γ reversion was estimated to be nearly completed at this temperature, irrespective of cold rolling reduction. Holding for slightly longer duration of 10 s, however, did not show

appreciable change in grain size (0.95 μm; Figure 4f). Some deformed original austenite grains were also found coexisting with the reverted grains. Rajasekhara et al. [9] reported that samples annealed at 800°C exhibited a rapid grain growth from ~ 0.5 μm to ~ 2.4 μm when the annealing duration was increased from 1 to 100 s due to high driving force for the grain growth.

Conclusions

Besides martensitic laths, stacking fault bundles are readily seen in deformed austenite at both 45% and 62% CR reductions; but the occurrence of these faults decreases on annealing at 800°C. Twinned martensite and microtwins in deformed austenite are occasionally observed in 45% CR specimen annealed at 730°C.

α'- γ reversion occurs primarily by nucleation and growth of fine austenite grains at martensite lath boundaries. A second type of nucleation mechanism, where reverted intralath γ layers form as thin plates traversing the martensitic laths, is also possible, as has been observed in a 45% CR specimen annealed at 730°C for 1 s.

The diffusion rate operating in cold rolled and reversion-annealed EN 1.4318 steel is extremely fast and the size of the reverted new austenite fine grains at 730°C/1 s annealing decreases with the cold rolling reduction, obviously due to an increased number of nuclei in deformed martensite.

Annealing at 800°C for 1 s resulted in nearly complete α'- γ reversion and the reverted grain size varied in a narrow range (0.8-1.1 μm) regardless of cold rolling reduction until about 10 s holding.

References

[1] P-J. Cunat, and T. Pauly, 4th European Stainless Steel Science and Market Congress, Association Technique de la Siderurgie Francaise, Paris, 1, 2002, p. 10.

[2] M.C. Somani, L.P. Karjalainen, M. Koljonen, P. Aspegren, T. Taulavuori, and A. Kyröläinen, 5th European Stainless Steel Science and Market Congress, eds. J.A. Odriozola, and A. Paul, Seville, Spain, 2005, p. 37.

[3] M. Somani, P. Karjalainen, P. Juntunen, S. Rajasekhara, P. Ferreira, A. Kyröläinen, T. Taulavuori, and P. Aspegren, International Symposium on Ultrafine Grained Structures 2005 (ISUGS 2005), Sanya, China, 2005, p. 283.

[4] M.C. Somani, L.P. Karjalainen, A. Kyröläinen, and T. Taulavuori, Mater. Sci. Forum, 539-543, 2007, pp. 4875-4880.

[5] P. Juntunen, M. Somani, P. Karjalainen, D. Misra, and A. Kyröläinen, International Symposium on Advances in Stainless Steels, Chennai, India, 2007.

[6] K. Tomimura, S. Takaki, and Y. Tokunaga, ISIJ Int., 31, 12, 1991, pp. 1431-1437.

[7] K. Tomimura, S. Takaki, S. Tanimoto, and Y. Tokunaga, ISIJ Int., 31, 7, 1991, pp. 721-727.

[8] S. Takaki, K. Tomimura, and S. Ueda, ISIJ Int., 34, 6, 1994, pp. 522-527.

[9] S. Rajasekhara, Development of Nano/Sub-micron Grain Structures in Metastable Austenitic Stainless Steels, The University of Texas at Austin, PhD thesis, 2007, p. 110.

[10] J. Talonen, and H. Hänninen, Acta Materialia, 55, 2007, pp. 6108-6118.

[11] M. Farooque, H. Ayub, A. Ul. Haq, and A.Q. Khan, J. Mater. Sci., 33, 11, 1998, pp. 2927-2930.

[12] T. Sourmai, Mater. Sci. Technol., 17, 1, 2001, pp. 1-14.

[13] S. Rajasekhara, P.J. Ferreira, L.P. Karjalainen, and A. Kyröläinen, 6th European Stainless Steel Conference - Science and Market, Helsinki, Finland, 2008 (in press).

ADVANTAGES AND CHALLENGES OF TEMPER ROLLED STAINLESS STEELS

M. Sellman, T. Taulavuori, P. Vainio

Tornio Research Centre, Outokumpu Tornio Works, Finland

Abstract

The successful utilization of temper rolled austenitic stainless steels necessitates knowledge and experience in the production of the material and in the end product manufacturing due to the special material properties. In this paper, not only the fascinating material properties of temper rolled stainless steels, but also few substantial facts in the production and end product manufacturing are presented.

Introduction

By using temper rolled austenitic stainless steels, it is possible to combine high strength, good formability and corrosion resistance. After temper rolling, the austenitic stainless steels still have ductility left, which is one of the most important properties. Additionally, temper rolling also hardens the surface and enhances abrasion resistance of the material. High strength enables lightweight structures and allows increased payloads. The demands of the end product must be recognised to make successful material choices and to utilize all the fascinating properties of the high strength stainless steels.

Temper rolling

In temper rolling, the applied thickness reduction has the strongest influence on the mechanical properties. Anyhow, in the production, there are also many other factors, which have a great impact on the properties and on the quality of these products. Therefore, routes are adjusted in detail for each specific case. At first, in the cold rolling mill, hot strips are rolled to an intermediate thickness, if the final thickness or customer specific surface requirements provide that. The higher the thickness reduction to the intermediate thickness in the cold rolling mill is, the smoother the surface of the end product. After rolling to the intermediate thickness, an intermediate annealing step adjusts the proper grain size and restores the isotropic mechanical properties. After annealing and descaling, the temper rolling is carried out with proper reduction to achieve the target mechanical properties. If flatness problems occur, the levelling machine can be used to straighten the material. After this, the coil is cut and slit to the dimensions requested by the customer.

Factors affecting material properties

The most important factors affecting material properties are the grain size, the alloying elements and the work hardening. The smaller grain size not only strengthens the steel due to greater amount of grain boundaries hindering the movement of dislocations, but also improves ductility. The alloying elements influence the strength by controlling the phase stability and the initial strength level of the annealed steel. The more unstable the material, the more martensite is

formed during work hardening. The martensite fraction as a function of cold rolling reduction is presented in Figure 1 for some austenitic stainless steel grades. In Figure 2, the work hardening curves for a stable and an unstable austenitic stainless steel are presented. [1]

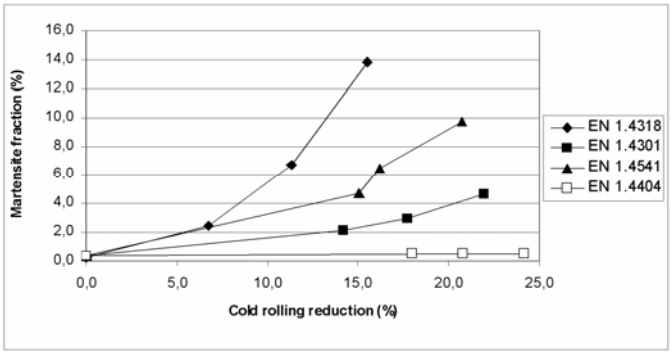

Figure 1. Martensite fraction as a function cold rolling reduction for austenitic stainless steels.[1]

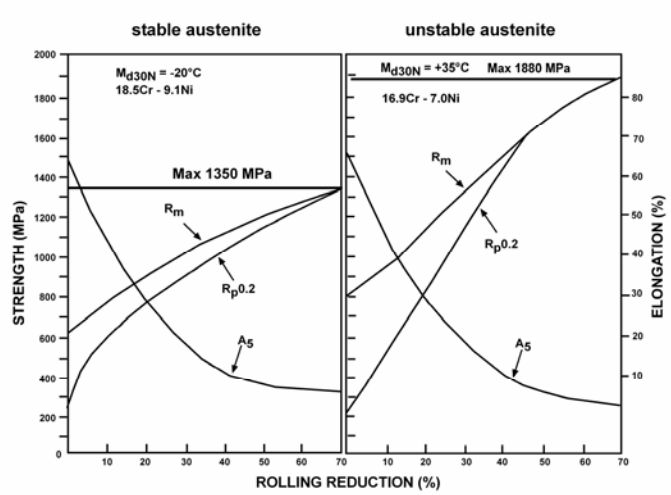

Figure 2. The effect of rolling reduction on mechanical properties for stable (on the left) and unstable (on the right) austenitic stainless steels are presented. [2]

The maximum temper rolling reduction is restricted by the work hardening rate, by the dimensions of rolled material and by the production limitations like for example maximum rolling forces and thickness limitations. Even though higher reductions would be attainable due to sufficient rolling forces, flatness may be the limiting factor. Adjusting the crowning and bending of the rolls, improves flatness. Within thin materials, the martensite fraction on the surface causes relatively high residual stresses, causing flatness problems. The final strength values are very sensitive to thickness variations, because a few hundredths of a millimeter may correspond to several percentage points in temper rolling reduction. Therefore, a high quality technology is needed when producing temper rolled thin materials.

Mechanical properties of temper rolled austenitic stainless steels

Temper rolled austenitic stainless steels possess high strength properties combined with relatively good elongation. For example, in temper rolled condition the steel grade 1.4310 (AISI 301) may have a 0.2% proof strength as high as 1900 N/mm^2 and a tensile strength of 2200 N/mm^2. In Figure 3 some examples of strength properties as a function of achieved A_5-elongation are presented for the steel grade 1.4318 (AISI 301LN). In addition, martensite formation is increased in the vicinity of the surface, hardening it more than the core and making

thin products more sensitive to flatness problems due to higher residual stresses. In Figure 4 the hardness profile determined with Vickers hardness test (HV10) and low-force (HV1) Vickers hardness test (HV1) and the martensite fraction are presented as a function of thickness for the steel grade 1.4318 in temper rolled condition 2H+C850 having the tensile strength between 850 – 1000 N/mm^2. [3]

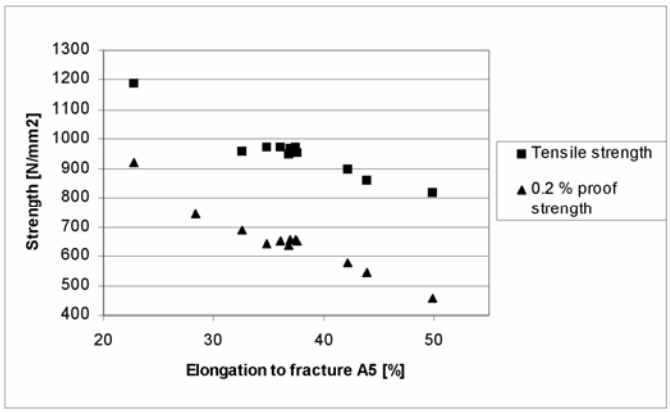

Figure 3. 0,2% proof strength and tensile strength as function of elongation for the steel grade 1.4318 (AISI 301LN).

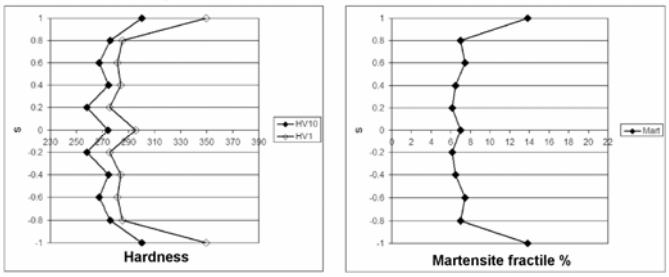

Figure 4. Hardness profile and martensite fractile as function of thickness for steel grade 1.4318 2H+C850. [3]

Anisotropy

The anisotropic behaviour is typical for temper rolled materials. The strength values measured transversal to the rolling direction are a little higher than the values measured longitudinal to the rolling direction. However, the Young's modulus remains the same, irrespective of the measuring direction. According to the "Design Manual for Structural Stainless Steel, Third Edition" due to anisotropy the characteristic value for design strength should be taken as 0.8 x minimum 0.2% proof strength for structural applications, where compression in the longitudinal direction is a relevant stress condition and a higher value may be used if supported by appropriate experimental data. [4,5]

Asymmetry

The yield strengths in tension and compression differ from each other. In addition, the difference depends on the rolling direction. Parallel to the rolling direction the yield strength in the tensile test achieves higher values than in the compression test. On the other hand, in the transverse direction the yield strength in the tensile test achieves a lower value than in the compression test. In Figure 5 some typical yield strength values both in the tensile test and the compression test are presented for the steel grade 1.4318 in temper rolled condition 2H+CP500 having the 0,2% proof strength between 500-700 N/mm^2.

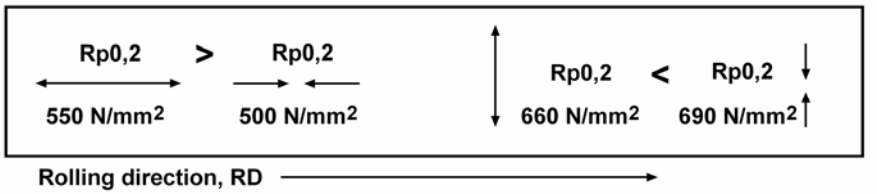

Figure 5. The 0.2% yield strength values of tensile test and compression tests measured parallel and perpendicular to the rolling direction for the steel grade 1.4318 2H+CP500.

Standards

European standard EN 10088-2 “Stainless steels – Part 2: Technical delivery conditions for sheet/plate and strip of corrosion resisting steels for general and construction purposes” classifies the strength classes either according to the tensile strength or according to the 0.2%-proof strength giving no minimum elongation values for each strength class. On the contrary, ASTM A666 specifies the nominal values for 0.2%-proof strength, tensile strength and minimum elongation for each strength class for specific thicknesses. Therefore, material delivered according to ASTM A666 is more strictly specified than according to EN 10088-2 [6,7]

Standards for applications

Rules concerning the structural use of temper rolled austenitic stainless steels have been included in the standard EN 1993-1-4 “Eurocode 3 part 4: Design of steel structures: General rules: Supplementary rules for stainless steels”. The temper rolled stainless steels can be used up to an undefined strength level, if dimensioning is justified according to Section 7 of the standard mentioned above. Also, the handbook “Design manual for Structural Stainless Steel” recommends that the cold worked stainless steels can be used in supporting structures up to strength levels +CP500 / +C850 having the 0,2% proof strength between 500-700 N/mm^2 and having the tensile strength between 850 – 1000 N/mm^2. So far, only the strength level of the base material in the annealed condition can be exploited in the heat affected zone of the weld. Cold worked stainless steels are not approved for pressure equipment applications but the possibility to obtain PMA (Particular Material Appraisal) exists for a defined pressure equipment application according to the Pressure Equipment Directive.

End product manufacturing

High strength austenitic stainless steels posses extremely good mechanical properties with a high elongation to fracture. However, some topics have to be taken into account when further processing is made.

Cutting

The cutting of temper rolled austenitic stainless steels is more demanding, compared to the soft annealed condition. Basically, the cutting forces are proportional to the tensile strength. However, it is supposed that the forces do not increase linearly in case of temper rolled stainless steels because the austenitic stainless steels in the soft annealed condition also work harden during cutting. On the other hand, the increased surface hardness of the temper rolled stainless steels has a great influence on tool wear. Horizontal clearance of the blades has to be larger than for stainless steel in the soft annealed condition to achieve a good quality cutting edge and to reduce the tool wear by decreasing the cutting forces. Blades should have sufficient combination of hardness and ductility due to the relatively good elongation properties of temper rolled stainless steels. [8]

Forming

The increase in the initial yield strength increases the forces needed in deep drawing processes. The higher strength can also be a limitation for the most demanding forming processes. Nevertheless, the Erichsen Index, describing the ability of the material to resist stretch forming, is not dramatically decreased with increasing yield strength, Figure 6.

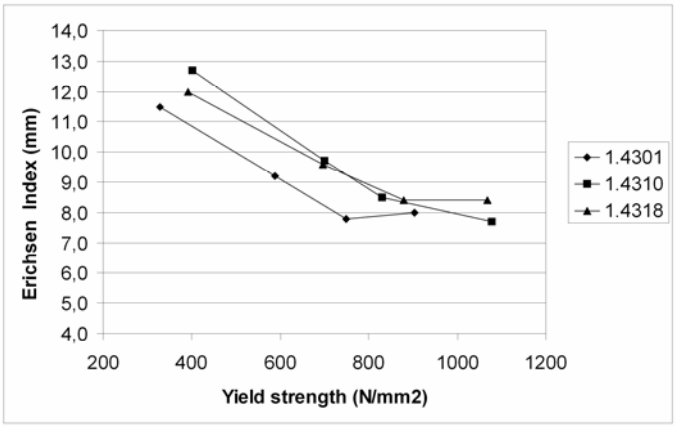

Figure 6. Erichsen Index measured for some austenitic steel grades in various strength levels.

Welding

In many cases the manufacturing of the end product includes welding, in which some softening effect occurs due to high heat input. The higher the strength properties are, the more dramatic is the softening in the heat affected zone. The width of this zone depends on the welding method. In figure 7 the hardness profile of the welded joints made by laser welding and by pulsed TIG-welding are presented for the steel grade 1.4301 at different strength classes. It can be clearly seen that the low heat input of the laser gives a clear benefit by decreasing the width of the softened region when compared to conventional fusion welding. [9]

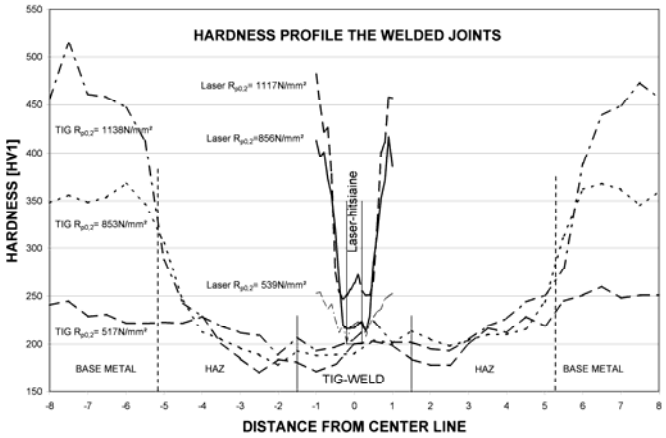

Figure 7. The hardness profile of laser and pulsed-TIG welded joints for the steel grade 1.4301 in thickness of 1.5mm. [9]

Successful applications

The temper rolled grades produced by Outokumpu have been utilized in structural components of cargo-vehicles, in lightweight structures, in load-bearing constructional elements, in honeycomb structures, in bus structure applications, in trucks and trains, in pharmaceuticals, in telecom applications etc. Also, shielding rings of beer kegs have turned out to be a successful application. In Figure 8 one application made of temper rolled stainless steel is presented.

Figure 8. Temper rolled materials are utilized innovatively, for example in this truck trailer construction made by Obas Oy.

References

[1] J. Salmén: “The anisotropic behaviour of the mechanical properties in hard cold rolled austenitic stainless steels”, Master’s Thesis (in Finnish), University of Oulu, Finland, 2004.

[2] A. Kyröläinen: High strength stainless steels – temper rolled, International Symposium on Advanced in Stainless Steels 2007, ISAS 2007,Chennai, India, 2007.

[3] P. Juntunen: ”Muokkaamalla lujitettujen ruostumattomien terästen muovattavuus Erä 1: kovuus ja martensiittipitoisuus nauhojen paksuussuunnassa sekä viivästyneet murtumat”, University of Oulu, internal report, Oulu, 2006.

[4] T. Taulavuori, P. Aspegren, J. Säynäjäkangas, J. Salmén, P. Karjalainen: The anisotropic behaviour of the nitrogen alloyed stainless steel grade 1.4318, High Nitrogen Steels Congress 2004, Ostend, Belgium, 2004.

[5] Design Manual For Structural Stainless Steel - Third Edition, Euro Inox and The Steel Construction Institute, Brussels, Belgium, 2006.

[6] EN 10088-2: Stainless steels – Part 2: Technical delivery conditions for sheet/plate and strip of corrosion resisting steels for general and construction purposes, 2005.

[7] ASTM A666 Standard Specification for Annealed or Cold-Worked Austenitic Stainless Steel Sheet, Strip, Plate and Flat Bar , 2003.

[8] P. Mikkonen: ”Pyöröleikkauksen eri tekijöiden vaikutus levyn ja nauhan leikkauksessa”, Master’s thesis (in Finnish), University of Oulu, 1989.

[9] A. Kyröläinen, J. Lukkari: Ruostumattomat teräkset ja niiden hitsaus. 2.painos.MET-julkaisuja nro 14/2002. Tampere

STUDIES ON STAINLESS STEELS AT THE UNIVERSITY OF OULU

L.P. Karjalainen

University of Oulu, Finland

In the Materials Engineering Laboratory of the University of Oulu research on stainless steels started as early as 1972. At that time the design of the first nuclear power station was topical in Finland, and one of the numerous topics investigated was the welding of tubes and pipelines for the secondary circuits, made of a Russian Ti-stabilized austenitic stainless steel. Also, the present author was involved, as a fresh researcher, in this research project, performing studies on the formation of delta-ferrite in welding and its measuring techniques [e.g. 1,2]. In the following years, extensive studies were carried out concerning especially the hot cracking risk in welding of austenitic stainless steels, and the concept of solidification mode and its importance in controlling the hot cracking susceptibility was pointed out by Suutala, Moisio and Takalo in several publications [see e.g. 3]. A few years later, Kujanpää finished his doctoral thesis dealing with welding defect formation in high-speed welding of austenitic stainless steel strips (such as in tube production), also closely related to the solidification mode [4]. Then, Leinonen investigated factors affecting the variation of the weld penetration in welding of austenitic stainless steels, showing the role of inclusions in addition to the sulphur content [5,6]. One project among the work on the weldability aspects of austenitic stainless steels dealt with the MMA, TIG and MIG welding of highly corrosion resistant 6%Mo bearing steel, mainly with shielding gas (N_2 additions) and filler selections (Nb-free 9%Mo alloy) [7,8]. In addition to weldability studies, some work on the corrosion properties of welded joints was conducted, as well [9,10].

After the establishment of Outokumpu stainless steel company and its plant in Tornio about 140 km north from Oulu, the research was fast directed from welding metallurgy to processing aspects of steels, the manufacturing stages (hot rolling and annealing, later the RAP-process), simulated by a Gleeble simulator. Processing of ferritic stainless steels (17%Cr-grade in particular) was an early topic [11,12]. Among ferritic stainless steels, another grade was the 12Cr-steel steel, its processing route [13-15] and also weldability aspects [16,17]. It was shown that the impact toughness in the heat-affected zone was excellent, if the chemical composition was balanced properly to avoid any delta-ferrite. Also the texture and formability of ferritic stainless steels, affected by the processing route, were investigated [18,19]. Furthermore, studies on duplex stainless steels were conducted, related with cracking problems in the hot rolling stage [20,21].

Strengthening of austenitic stainless steels has been a target already for 15 years. A conventional route is temper rolling of the annealed steels and the mechanical properties [22,23] obtained and the influence of welding on the heat affected zone of strengthened steels have been topics under investigations, in addition to the delayed cracking risk in tubes and formed components. Recently, the various strengthening methods are discussed in a review paper under printing [24].

An interesting concept is the utilization of martensite reversion to obtain ultra fine-grained austenite. This route was investigated with Outokumpu company and two American universities at Austin and Lafayette. Several conference and journal papers have been published on the basis of the research performed [e.g. 25-28], and four presentations will still be given in this conference.

Another special approach is the grain boundary engineering and as applied to austenitic stainless steels it may be utilized in improving certain mechanical and corrosion properties. Some thermo-mechanical treatments have been applied and found successful to increase the number of low-sigma coincidence grain boundaries.

Participation and contributing in stainless steels conferences since the year 1991 in Chiba, Japan, until Helsinki 2008 has been quite regular and continuous [e.g. 8,12,15,16,17,19, 20,23,25,29,30]. The research group has also participated in several European research projects on stainless steels, funded by ECSC and RFCS, since 1995 when it became possible for Finnish participants, in cooperation with Acerinox SA, RWTH Aachen, Labein, etc.

Acknowledgements

The funding received over several decades from Outokumpu Stainless Oy, Outokumpu Foundation, The Finnish Agency for Technology and Innovation (Tekes) and ECSC/RFCS is acknowledged with gratitude.

References

[1] P. Karjalainen, T. Takalo and T. Moisio, Hitsaustekniikka (Welding technology), 23, No.6, (1973) 146-152 (in Finnish).
[2] *ibid*, Hitsaustekniikka (Welding technology), 24, No.5 (1974) 172 - 178 (in Finnish).
[3] N. Suutala, “Solidification studies on austenitic stainless steels”, Acta Universitatis Ouluensis, Series C, Technica No. 23, Doctoral thesis, 1982, University of Oulu.
[4] V. Kujanpää, “Studies on weld defects in austenitic stainless steels”, Acta Universitatis Ouluensis, Series C, Technica No. 28, Doctoral thesis, 1984, University of Oulu.
[5] J. Leinonen, “Cast-to-cast variations in weld petetration in austenitic stainless steels”, Acta Universitatis Ouluensis, Series C, Technica No. 39, Doctoral thesis, 1987, University of Oulu.
[6] J.I. Leinonen, S.A. Järvenpää, and L.P. Karjalainen, ”Harmful effect of calcium on weld penetration characteristics”. Proceedings of the 3rd International Conference on Trends in Welding Research, Gatlinburg, Tennessee, 1-5 June 1992. pp. 713 - 717.
[7] L.P. Karjalainen, S.A. Järvenpää and J.I. Leinonen, ”Welding of Cr-Ni-6Mo-N type steels”, Proceedings of the International Conference on the Joining of Materials, JOM-5, Helsingör, Denmark, 1991, pp. 462 - 467.
[8] S.A. Järvenpää, J.I. Leinonen, L.P. Karjalainen, and N. Suutala, ”Impact toughness and pitting corrosion properties of metal arc, MIG and plasma welds in a 20Cr-22Ni-6Mo-N steel”. Proceedings of International Conference on Stainless Steels '91, Chiba, Japan, 10 - 13 June 1991. Vol. 1, pp. 379 - 386.
[9] A.I. Grekula, V.P. Kujanpää and L.P. Karjalainen, Corrosion, 40, No. 11 (1984) 569 - 572.
[10] P. Karjalainen and N. Suutala, Stainless Steel Industry, May 1991, 4 & 6.
[11] T. Kauppi, P. Karjalainen, and A. Kyröläinen, ”Influence of thermo-mechanical processing on microstructure and properties of a 17 % Cr ferritic stainless steel.” Proceedings of the

International Symposium on Physical Simulation, Delft, The Netherlands, 22 - 24 April 1992. pp. 125 - 129.
[12] T.A. Kauppi, L.P. Karjalainen, and A.J. Kyröläinen, “Influence of deformation and cooling rate on the gamma/delta transformation in low carbon AISI 430 ferritic stainless steel.” 1st European Stainless Steel Conference. Innovation Stainless Steel, Florence, Italy, 11 - 14 Oct. 1993. Vol. 2, pp. 333 - 338.
[13] L.P. Karjalainen, J.S. Perttula, and J.A. Koskiniemi, “Recrystallisation behaviour of 12% Cr ferritic stainless steels as revealed by the stress relaxation technique”. 2nd International Conference on Modelling of Metal Rolling Processes, London, UK, 9 - 11 Dec., 1996. (eds. J.H. Beynon et al.) Abingdon ,1996. pp. 324 - 333.
[14] J.A. Koskiniemi, L.P. Karjalainen, P.G.H. Pistorius, and G.T. van Rooyen, Mat. Sci. Techn., 14, No.11 (1998) 1115 - 1121.
[15] J.A. Koskiniemi, J.M. Prozzi, and L.P. Karjalainen, “The effects of chemical composition and hot rolling on the tempering kinetics of 12Cr stainless steels”. Intern. Congress: Stainless Steel ‘99 Science and Market: 3rd European Congress, 6 - 9 June 1999, Chia Laguna, Sardinia, Italy. Proceedings. Vol. 2. pp. 97 - 105.
[16] P. Karjalainen, A. Kyröläinen, T. Kauppi, and U. Orava, ”Mechanical properties and weldability of new 12Cr-type stainless steel sheets”. Applications of stainless steel '92, Stockholm, Sweden, 9 - 11 June 1992. (eds. H. Nordberg and J. Björklund), 1992. Vol. 1, pp. 225 - 234.
[17] U.H. Orava, L.P. Karjalainen, and A.J. Kyröläinen, ”Impact toughness of heat affected zone in non-stabilized 12% ferritic stainless steel welds”. 1st European Stainless Steel Conference. Innovation Stainless Steel, Florence, Italy, 11 - 14 Oct. 1993. Vol. 2, pp. 149 - 154.
[18] M. Ylitalo, ”Untersuchung des Einfluss der chemischen Zusammensetzung, der Warmbandverformung und der Warmbandgluhung auf die Verformbarkeit von ferritischen Edelstählen”, Acta Universitatis Ouluensis, Technica C 93, Doctoral thesis, 1996. University of Oulu.
[19] P. Juntunen, A. Kyröläinen, and P. Karjalainen, ”Effects of hot band annealing and cold rolling reduction on texture and plastic anisotropy of 12Cr-Ti ferritic stainless steels”. Intern. Congress, Stainless Steel ‘99 Science and Market, 3rd European Congress, 6 - 9 June 1999, Chia Laguna, Sardinia, Italy. Proceedings. Vol. 2. pp. 163 - 172.
[20] J.I. Kömi, Jukka and L.P. Karjalainen, “Effect of restoration kinetics on hot ductility of a ferritic-austenitic and super austenitic stainless steels”. Stainless Steels '96, June 3 - 5, 1996. Proceedings. Germany 1996. pp. 301 - 302.
[21] J.I. Kömi, ”Hot ductility of austenitic stainless steels under hot rolling conditions”, Acta Universitatis Ouluensis, Technica C 164, Doctoral thesis, 2001. University of Oulu.
[22] T. Taulavuori, P. Aspegren, J. Säynäjäkangas, J. Salmén and P. Karjalainen, “The anisotropic behaviour of the nitrogen alloyed stainless steel grade 1.4318”, Proc. Intern. Conf on High Nitrogen Steels 2004, (eds. N. Akdut, B.C. DeCooman, and J. Foct), (GRIPS Media), Sept.19-22, 2004, Oodense, Belgium, pp. 405-409.
[23] R. Tarkiainen, R. Levonmaa, and P. Karjalainen, ”The effect of nitrogen on the hardness of martensite phase and strength of AISI 301LN temper-rolled stainless steels”. Applications of stainless steel '92, Stockholm, Sweden, 9-11 June 1992. (eds. H. Nordberg and J. Björklund). Kristianstad 1992. Vol. 1, pp. 43 - 52.
[24] L.P. Karjalainen, T. Taulavuori, M. Sellman, and A. Kyröläinen, ”Some Strengthening Methods for Austenitic Stainless Steels”, Steel Research Intern., Special Issue on Stainless Steels, in printing.

[25] M.C. Somani, L.P. Karjalainen, M. Koljonen, P. Aspegren, T. Taulavuori and A. Kyröläinen, ”Microstructure and mechanical properties of reversion annealed cold-rolled 17Cr-7Ni type austenitic stainless steels”, Stainless Steel´ 05, Proc. the 5th European Congress, Stainless Steel Science and Market, (eds. J.A. Odriozola and A. Paul), Seville, Spain, Sept. 27-30, 2005, pp. 37-42.
[26] M. Somani, P. Karjalainen, P. Juntunen, S. Rajasekhara, P. Ferreira, A. Kyröläinen, T. Taulavuori and P. Aspegren, ”Submicron microstructure and mechanical properties achieved in a short annealing of cold-rolled austenitic stainless steels”, Iron & Steel, Supplement, 40, (2005) 283-289. (The Joint Intern. Conf. of HSLA Steels 2005 and ISUGS 2005 Proceedings).
[27] M.C. Somani, L.P. Karjalainen, A. Kyröläinen and T. Taulavuori, ”Processing of submicron grained microstructures and enhanced mechanical properties by cold-rolling and reversion annealing of metastable austenitic stainless steels”, Materials Science Forum, 539-543, (2007) 4875-4880.
[28] S. Rajasekhara, P.J. Ferreira, L.P. Karjalainen, and A. Kyröläinen, Metall. Mater. Trans. A, 38A, No.6, (2007) 1212-1210.
[29] M-S. Kantanen, P. Karjalainen, and T. Kauppi, “Softening behaviour of austenitic stainless steels in simulated continuous annealing”. International Congress: Stainless Steel ‘99 Science and Market: 3rd European Congress, 6 - 9 June 1999, Chia Laguna, Sardinia, Italy. Proceedings. Vol. 2. pp. 173 - 181.
[30] R. Sanchez, V. Matres, J. Botella, M. Barteri, C. Merino, A. Pardo, and P. Karjalainen, ”Low nickel austenitic stainless steel with high pitting corrosion resistance”, 4th European Stainless Steel Science and Market Conference, Paris 10-13 June, 2002, vol. 2, p. 56 - 61.